Journal of Applied Mathematics and Physics, 2025, 13(12), 4506-4547
https://www.scirp.org/journal/jamp
ISSN Online: 2327-4379
ISSN Print: 2327-4352

Numerical Analysis of Approximate Solutions and Linear Growth in a Glial Cell Dynamics Model

Somayyeh Azizi*

Independent Researcher, Sendai, Japan
Email: *somayeh_azizi82@yahoo.com

How to cite this paper: Azizi, S. (2025) Numerical Analysis of Approximate Solutions and Linear Growth in a Glial Cell Dynamics Model. *Journal of Applied Mathematics and Physics*, **13**, 4506-4547.
https://doi.org/10.4236/jamp.2025.1312248

Received: February 19, 2025
Accepted: December 21, 2025
Published: December 24, 2025

Abstract

In this study, we investigate a mathematical model that describes the growth dynamics of glial cells in glioma, formulated as a nonlinear partial differential equation with a treatment-dependent source term. To approximate the solution of this model, we employ three semi-analytical techniques: the Homotopy Analysis Method (HAM), the Homotopy Perturbation Method (HPM), and the Reduced Differential Transform Method (RDTM). A comparative analysis shows that while all three methods produce accurate results, RDTM exhibits rapid stabilization across various time points, outperforming HAM and HPM in terms of convergence speed and computational efficiency. To incorporate memory effects commonly observed in biological systems, we extend the model to a fractional-order framework. Within this extension, we apply HPM, the Fractional Reduced Differential Transform Method (FRDTM), and RDTM to construct higher-order approximations and examine their convergence behavior. We also conduct detailed convergence and error analysis for the resulting series of solutions, providing theoretical validation of their accuracy and reliability. The simulation results reveal a steady decline in glial cell concentration over time, eventually approaching negligible levels, indicating effective suppression of glioma growth under the modeled treatment. Notably, smaller values of the fractional-order parameter accelerate this decline, highlighting the significant influence of fractional dynamics on treatment outcomes. Finally, we establish the existence, uniqueness, and stability of the solution using the sectorial operator framework and the Mittag-Leffler function representation, reinforcing the mathematical soundness of the proposed model. These findings underscore the potential of fractional modeling and semi-analytical methods in capturing the complex behavior of glioma progression and enhancing therapeutic strategies.

Keywords

Nonlinear Equation, Glial Cells, Numerical Methods, Fractional Diffusion Equation, Approximate Solution

1. Introduction

Brain development continues for several years after birth, largely due to the presence and activity of glial cells. These cells provide essential physical and chemical support to neurons, help maintain the neural environment, and play a critical role in the central nervous system (CNS). However, glial cells are also closely associated with various CNS disorders. When they grow uncontrollably, they can disrupt normal brain development and function. One such disorder is glioma, a type of tumor caused by the over proliferation of glial cells. When glioma occurs in children, it is referred to as pediatric glioma [1]. This neurological condition is typically treated through a combination of chemotherapy, radiotherapy, and surgical intervention [2]. In recent years, mathematical modeling has emerged as a powerful tool for understanding the complex biological dynamics of the brain and its disorders [3]-[6]. These models allow researchers to analyze biological problems, formulate and test hypotheses, and gain deeper insights into the mechanisms underlying disease progression and treatment response. A foundational mathematical formulation of the glioma model was introduced by Wein and Koplow [7], governed by a second-order partial differential equation, expressed as:

$$\begin{aligned}\frac{\partial u(r,\tau)}{\partial t} &= D\nabla^2 u(r,\tau) + p(\tau)n - k(\tau)n \\ &= D\frac{1}{r^r}\frac{\partial}{\partial r}\left(r^r \frac{\partial u(r,\tau)}{\partial r}\right) + p(\tau)u(r,\tau) - k(\tau)u(r,\tau),\end{aligned} \tag{1.1}$$

in this equation, the parameters $u(r,\tau)$, D, ∇^2, and k represent, respectively: the concentration of glioma cells as a function of time τ and radial distance r; the diffusion coefficient estimating the areal speed of invasive glioblastoma cells; the Laplacian operator; and the net rate of glial cell growth and killing. This model describes the spatiotemporal evolution of glioma density in the absence of treatment. Notably, earlier two-dimensional models had also been proposed [8] [9]. Interestingly, research by Stipe *et al.* [10] suggests that certain treatments such as combined radiotherapy and chemotherapy may paradoxically contribute to glioma growth. In response to these findings, Bernal and González-Gaxiola [11] proposed a modified glioma model in 2015, introducing a treatment parameter to account for therapeutic effects. Their updated formulation, detailed in Section 2, incorporates a nonlinear term $\omega(r,\tau)$ to model the suppression of glioma growth under treatment.

This study conducts a numerical analysis of the modified model, aiming to capture the approximate linear progression of glial cell concentration during treatment. To evaluate the effectiveness of various semi-analytical methods in solving

nonlinear partial and fractional differential equations relevant to glioma dynamics, we employ the Homotopy Analysis Method (HAM), Homotopy Perturbation Method (HPM), and Reduced Differential Transform Method (RDTM). The approximate solutions generated by these methods are illustrated in **Figure 1**, providing a basis for comparative analysis of their convergence behavior and accuracy. The figure also showcases the linear growth profile produced by RDTM at various time points, emphasizing its rapid stabilization relative to HAM and HPM. The influence of medical treatment parameters on the spatial spread of glial cells is illustrated in **Figure 2**, where the radius of cell concentration is shown to decrease over time.

As a continuation of this investigation, we further examine the role of fractional derivatives in shaping the concentration dynamics of glioma cells by extending the model to a time-fractional reaction-diffusion framework, as introduced in [12]. This extension enables the incorporation of memory effects and anomalous diffusion behaviors frequently observed in biological systems. To solve the fractional model, we implement the Homotopy Perturbation Method (HPM) using two distinct strategies: direct recursive expansion and an embedding parameter formulation involving Mittag-Leffler functions. Additionally, the Fractional Reduced Differential Transform Method (FRDTM) and the Reduced Differential Transform Method (RDTM) are employed to provide a consistent and comparative evaluation of solution performance within this extended context. Our analysis is grounded in the Caputo-type fractional diffusion equation, which serves as the mathematical foundation for modeling the time-dependent behavior of glioma cell concentration under fractional-order dynamics. To ensure the reliability of the obtained solutions, we conduct a thorough investigation of their convergence properties and provide error estimates for all series solutions. The impact of varying fractional orders is illustrated in **Figures 3-5**, which display solution profiles and line graphs capturing the system's evolving dynamics. In addition to the numerical analysis, we also establish the existence, uniqueness, and continuous dependence of the solution to the fractional model. This is achieved through three complementary analytical approaches: the fixed-point method via the fractional Volterra formulation, the spectral semigroup approach involving Mittag-Leffler functions, and the Laplace transform technique. Each method verifies that the problem is well-posed within suitable functional spaces. These theoretical properties are visually supported in **Figure 6**, which illustrates the stability and structure of the solution space under the fractional framework, reinforcing the mathematical soundness of the model.

2. Mathematical Formulation of a Treated Glioma Model

Roberto Bernal *et al.* (see [11] again) proposed an advanced mathematical framework to describe the spatiotemporal evolution of glioma cell proliferation. This model extends the classical diffusion-reaction paradigm by incorporating spatial and temporal heterogeneity, capturing the complex biological behavior of glioma

growth more accurately. Traditional models often assume constant diffusion and linear reaction kinetics, which fail to reflect the invasive and proliferative nature of gliomas, especially under the influence of treatment. To address these limitations, Bernal and colleagues introduced a modified partial differential equation (PDE) with variable diffusion and nonlinear reaction terms:

$$\frac{\partial u(r,\tau)}{\partial \tau} = D(r,\tau)\left(\frac{\partial^2 u}{\partial r^2} + \frac{2}{r}\frac{\partial u}{\partial r}\right) + \left[p(\tau) - k(\tau)\right]u(r,\tau) \tag{2.1}$$

Here, $u(r,\tau)$ represents the glioma cell density at radial position $r \geq 0$ and time $\tau \geq 0$. The diffusion coefficient $D(r,\tau)$, proliferation rate $p(\tau)$, and decay rate $k(\tau)$ may vary with space and time. The term $\frac{2}{r}\frac{\partial u}{\partial r}$ arises from the Laplacian in spherical coordinates, assuming radial symmetry. The initial condition is:

$$u(r_0,\tau_0) = N_0$$

where r_0 is the initial tumor radius, τ_0 is diagnostic time, and N_0 is the initial cell density. In follow-up studies by Carpio and Bonilla [13] [14], the model was simplified by assuming constant diffusion D and no decay $k(\tau) \equiv 0$, yielding a linear diffusion-reaction equation:

$$\frac{\partial u}{\partial \tau} = D\left(\frac{\partial^2 u}{\partial r^2} + \frac{2}{r}\frac{\partial u}{\partial r}\right) + pu$$

This equation admits a Gaussian solution:

$$\eta(r,\tau) = \frac{N_0 \exp\left(p\tau - \frac{r^2}{4D\tau}\right)}{(8\pi D\tau)^{3/2}} \tag{2.2}$$

The denominator reflects three-dimensional diffusion, while the exponential decay term models spatial attenuation from the tumor core. To simplify further, Bernal *et al.* introduced a time rescaling $\tau = 2Dt$ and defined the normalized net proliferation rate:

$$\omega(r,\tau) = \frac{p(\tau) - k(\tau)}{2D}$$

Assuming D is constant and ω is independent of τ, the solution becomes:

$$N(r,\tau) = N_0 \exp\left(\omega(r)(\tau - \tau_0)\right) \cdot \exp\left(-\frac{r^2}{2(\tau - \tau_0)}\right)$$

If ω varies with time, the exponential must be replaced by an integral:

$$\exp\left(\int_{\tau_0}^{\tau} \omega(r,s)\,\mathrm{d}s\right)$$

To isolate nonlinear behavior, the diffusion coefficient is fixed at $D = \frac{1}{2}$, yielding:

$$\frac{\partial u}{\partial \tau} = \frac{1}{2}\frac{\partial^2 u}{\partial r^2} + \omega(r,\tau)$$

Here, $\omega(r,\tau)$ acts as a source term. To model treatment effects, Bernal *et al.* proposed a nonlinear form:

$$\omega(r,\tau) = \mathrm{e}^{-u} + \frac{1}{2}\mathrm{e}^{-2u}$$

This reflects increased treatment efficacy at lower cell densities. Substituting into the PDE gives the final nonlinear equation:

$$\frac{\partial u}{\partial \tau} = \frac{1}{2}\frac{\partial^2 u}{\partial r^2} + \mathrm{e}^{-u} + \frac{1}{2}\mathrm{e}^{-2u} \tag{2.3}$$

The initial condition is:

$$u(r,0) = \ln(r+2).$$

This ensures a smooth, positive initial profile and avoids singularities at $r = 0$. This nonlinear parabolic PDE presents analytical and numerical challenges due to its nonlinearity and spatially dependent initial condition. Standard linear techniques are insufficient, necessitating numerical methods such as finite difference or spectral schemes. The model exhibits rich dynamics due to the interplay between diffusion and nonlinear reaction, enabling the study of complex tumor behaviors. Finally, the treated glioma radius is given by (see also [11]):

$$r_{\text{treated}} = \mathrm{e}^{N_0} - \tau - 2 \tag{2.4}$$

This expression links the tumor radius to time and initial density, offering a practical metric for evaluating treatment outcomes.

3. Preliminaries

3.1. Basic Idea of the Homotopy Analysis Method (HAM)

One of the most widely used non-perturbative analytical techniques is the Homotopy Analysis Method (HAM), originally proposed by Shi-Jun Liao [15]-[17]. HAM is a powerful and flexible approach for solving both linear and nonlinear differential and integral equations. It blends traditional perturbation techniques with the concept of homotopy from topology, providing a broader framework for constructing analytical solutions. Unlike classical perturbation methods, HAM does not rely on the presence of small or large parameters. Instead, it introduces a convergence-control parameter c, which allows researchers to adjust and regulate both the region and rate of convergence of the series solution [18]. This flexibility enables HAM to yield either exact closed-form solutions or rapidly converging series that approximate the exact solution with high accuracy.

To illustrate the fundamental idea of HAM, consider a general nonlinear differential equation:

$$N\left[u(r,t)\right] - f(r,t) = 0 \tag{3.1}$$

where N is a nonlinear operator and $u(r,t)$ is the unknown function. For

simplicity, boundary conditions are omitted, though initial conditions can be incorporated similarly. HAM constructs the zero-order deformation equation as follows [15]:

$$(1-q)L\left[u(r,t;q)-u_0(r,t)\right]=qcR(r,t)\left[N\left[u(r,t;q)\right]-f(r,t)\right] \tag{3.2}$$

In this equation, $q\in[0,1]$ is the embedding parameter, $c\neq 0$ is the convergence-control parameter, $u(r,t;q)$ is an unknown function, $u_0(r,t)$ is an initial guess of the solution, $R(r,t)$ is a nonzero auxiliary function, and L is an auxiliary linear operator.

When $q=0$ and $q=1$, Equation (3.2) yields:

$$u(r,t;0)=u_0(r,t), u(r,t;1)=u(r,t) \tag{3.3}$$

This shows that as q increases from 0 to 1, the solution continuously deforms from the initial guess $u_0(r,t)$ to the actual solution $u(r,t)$. By differentiating Equation (3.2) m-times with respect to q and then setting $q=0$, we obtain the m-th order deformation equation:

$$u_m(r,t)-\chi_m^* u_{m-1}(r,t)=cH(r,t)A_m(u_{m-1}) \tag{3.4}$$

where

$$A_m(u_{m-1})=\frac{1}{(m-1)!}\frac{\partial^{m-1}}{\partial q^{m-1}}\left[N\left[u(r,t;q)\right]-f(r,t)\right]\Big|_{q=0} \tag{3.5}$$

Assuming $H(r,t)=1$, the equation simplifies to:

$$u_m(r,t)=\chi_m^* u_{m-1}(r,t)+cI_t^{\alpha}\left[A_m(u_{m-1})\right] \tag{3.6}$$

Here, I_t^{α} denotes the fractional integral operator defined by:

$$I^{\alpha}u(t)=\frac{1}{\Gamma(\alpha)}\int_0^t (t-\tau)^{\alpha-1}u(\tau)\mathrm{d}\tau, t>0, \alpha>0$$

The switching function χ_m^* is defined as:

$$\chi_m^*=\begin{cases}0, & m\leq 1\\ 1, & m>1\end{cases} \tag{3.7}$$

For $m\geq 1$, each $u_m(r,t)$ is governed by a linear equation with boundary conditions derived from the original problem. Expanding $u(r,t;q)$ in a Taylor series with respect to q, we get:

$$u(r,t;q)=u_0(r,t)+\sum_{m=1}^{\infty}u_m(r,t)q^m$$

Setting $q=1$, the final solution becomes:

$$u(r,t)=u_0(r,t)+\sum_{m=1}^{\infty}u_m(r,t) \tag{3.8}$$

The set $\{u_m\}=\{u_0(r,t),u_1(r,t),\cdots,u_n(r,t)\}$ represents the components of the series solution.

3.2. Basic Idea of Homotopy Perturbation Method (HPM)

In recent years, the Homotopy Perturbation Method (HPM), originally proposed

by J.H. He [19]-[21], has emerged as an effective and versatile analytical technique for solving a broad class of linear and nonlinear functional equations. By integrating the classical perturbation approach with the topological concept of homotopy, HPM provides a robust framework for constructing both exact and approximate solutions. Its adaptability has led to successful applications in various domains, including fluid mechanics, heat transfer, biological systems, and nonlinear oscillatory phenomena. Compared to traditional perturbation methods, HPM typically involves fewer computational steps and yields highly accurate results, making it a valuable tool for both theoretical investigations and practical applications. To illustrate the fundamental idea of HPM, consider the general nonlinear differential equation

$$A(u)-f(r)=0, r\in D\subset\mathbb{R}^n, \tag{3.9}$$

subject to the boundary condition

$$B\left(u,\frac{\partial u}{\partial n}\right)=0, r\in\partial D, \tag{3.10}$$

where A is a general differential operator defined by the specific problem, B is a boundary operator, $f(r)$ is a known analytic function, and ∂D denotes the boundary of the domain D. The operator A is typically decomposed into a linear part L and a nonlinear part N, so that Equation (3.9) can be rewritten as

$$L(u)+N(u)-f(r)=0. \tag{3.11}$$

Following the homotopy technique introduced in [18], a homotopy $H(v,q):\Omega\times[0,1]\to\mathbb{R}$ is constructed in the form

$$H(v,q)=(1-q)\left[L(v)-L(u_0)\right]+q\left[A(v)-f(r)\right]=0, \tag{3.12}$$

where $q\in[0,1]$ is the embedding (homotopy) parameter and u_0 is an initial approximation of the solution. By setting $q=0$ and $q=1$, one obtains

$$H(v,0)=L(v)-L(u_0), \tag{3.13}$$

and

$$H(v,1)=A(v)-f(r)=0,$$

which corresponds to the original problem.
The solution v is expressed as a power series in q:

$$v=v_0+qv_1+q^2v_2+\cdots. \tag{3.14}$$

Substituting Equation (3.14) into the homotopy Equation (3.12) and equating terms with identical powers of q, a sequence of linear equations is obtained for the components $v_0,v_1,v_2,\cdots$. Setting $q=1$, the approximate solution to the original problem is given by

$$u(r,t)=\lim_{q\to1}v=v_0+v_1+v_2+\cdots. \tag{3.15}$$

This series converges with the exact or an approximate solution, depending on the nature of the problem and the choice of the initial approximation u_0.

3.3. Basic Idea of Reduced Differential Transform Method (RDTM) and Fractional RDTM (FRDTM)

The Reduced Differential Transform Method (RDTM) was first proposed by Zhou in 1986 [22]. Since then, it has garnered significant attention due to its successful application in solving a wide variety of problems [23] [24]. To illustrate the basic concepts of this method, consider a function $u(r,t)$ that is analytic and continuously differentiable in the domain of interest. Based on the properties of the one-dimensional differential transformation, the function $u(x,t)$ can be represented as:

$$u(x,t)=\sum_{k=0}^{\infty}U_k(x)t^k$$

Here, $U_k(x)$ is called the *t-dimensional spectrum function* of $u(x,t)$. The basic definitions and operations of RDTM are reviewed as follows:

Definition 1: If the function $u(x,t)$ is analytic and continuously differentiable with respect to time t and space r in the domain of interest, then:

$$U_k(x)=\frac{1}{k!}\left[\frac{\partial^k}{\partial t^k}u(x,t)\right]_{t=0} \tag{3.16}$$

The differential inverse transform of $U_k(x)$ is defined as:

$$u(x,t)=\sum_{k=0}^{\infty}U_k(x)t^k \tag{3.17}$$

Combining Equations (3.16) and (3.17), we obtain:

$$u(x,t)=\sum_{k=0}^{\infty}\frac{1}{k!}\left[\frac{\partial^k}{\partial t^k}u(x,t)\right]_{t=0}t^k. \tag{3.18}$$

This method allows for highly accurate results or even exact solutions to differential equations.

- Fractional Reduced Differential Transform Method (FRDTM)

To broaden the scope of the Reduced Differential Transform Method (RDTM) to include fractional-order differential equations, Keskin and Oturanc developed the Fractional Reduced Differential Transform Method (FRDTM) in 2010 [25]. This technique has proven to be a reliable and efficient approach for finding approximate or exact solutions to fractional differential equations, which are often used to describe systems with memory effects and non-local behavior. The core principles of the one-dimensional fractional differential transformation are outlined as follows: Assume that $u(r,t)$ is a function of two variables that is analytic within a domain q, and let $(r,t)=(r_0,t_0)$ be a point in this domain. The fractional differential transformation of $u(r,t)$ is given by:

$$U(r)=\frac{1}{\Gamma(q\alpha+1)}\left[\frac{\partial^{q\alpha}}{\partial t^{q\alpha}}u(r,t)\right]_{t=0} \tag{3.19}$$

where α denotes the order of the fractional derivative. The differential inverse transform of $u(r,t)$ is given by:

$$u(r,t)=\sum_{q=0}^{\infty}U(r-r_0)^q(t-t_0)^q. \tag{3.20}$$

Combining Equations (3.19) and (3.20), we get:

$$u(x,t)=\sum_{q=0}^{\infty}\frac{1}{\Gamma(q\alpha+1)}\left[\frac{\partial^{q\alpha}}{\partial t^{q\alpha}}u(r,t)\right]_{t=0}t^{q\alpha}.$$

For functions of the form $u(r,t)=D_t^{n\alpha}u(r,t)$, the differential inverse transform is defined as:

$$u(r,t)=\sum_{q=0}^{\infty}\frac{\Gamma(q\alpha+1)}{\Gamma(q\alpha+\alpha+1)}\left[\frac{\partial^{q\alpha}u(r,t)}{\partial r^{\partial q\alpha}}\right]_{\substack{r=0\\t=0}}r^{q}t^{q}. \tag{3.21}$$

4. Approximate Solutions for the Treated Glioma Model

In this section, we investigate the nonlinear dynamics of glioma progression after therapeutic intervention by applying three powerful semi-analytical methods: the Homotopy Analysis Method (HAM), the Homotopy Perturbation Method (HPM), and the Reduced Differential Transform Method (RDTM). These techniques are employed to derive approximate solutions to a modified version of Equation (2.3), which incorporates a treatment-specific parameter to simulate the effects of therapy. By solving this enhanced model, we aim to understand how glioma cell concentrations change over time and space in response to treatment. Each method is evaluated not only for its ability to produce accurate approximations but also for its convergence behavior and effectiveness in capturing the decline in glial cell density at key spatial and temporal points. This comparative study offers valuable insights into the strengths and limitations of each approach, helping to identify the most suitable technique for modeling complex biological responses in post-treatment glioma dynamics.

4.1. Analytical Solution via the Homotopy Analysis Method

In this section, we apply the homotopy analysis method (HAM) to the nonlinear partial differential Equation (2.3)

$$\frac{\partial u}{\partial \tau}=\frac{1}{2}\frac{\partial^2 u}{\partial r^2}+\mathrm{e}^{-u}+\frac{1}{2}\mathrm{e}^{-2u},u(r,0)=\ln(r+2),$$

For $r\in\mathbb{R}$ (or $r\geq 0$ with appropriate boundary conditions; for concreteness, we proceed on $\mathbb{R}$ and discuss boundaries later). This equation is of reaction-diffusion type, with nonlinear source terms e^{-u} and e^{-2u}.

To facilitate the application of HAM, we define the nonlinear operator

$$N[u]=\frac{\partial u}{\partial \tau}-\frac{1}{2}\frac{\partial^2 u}{\partial r^2}-\mathrm{e}^{-u}-\frac{1}{2}\mathrm{e}^{-2u}.$$

We select the initial guess

$$u_0(r,\tau)\equiv\ln(r+2),$$

which satisfies the initial condition and is independent of τ. The auxiliary linear operator is chosen as

$$L[\phi]\equiv\frac{\partial \phi}{\partial \tau}-\frac{1}{2}\frac{\partial^2 \phi}{\partial r^2},$$

which is invertible under standard heat-equation solvability using a suitable Green's function. We introduce the convergence-control parameter $\hbar \in \mathbb{R} \setminus \{0\}$ and the embedding parameter $p \in [0,1]$. The zeroth-order deformation equation is constructed as

$$(1-p)L\left[\Phi(r,\tau;p)-u_0(r,\tau)\right]=p\hbar N\left[\Phi(r,\tau;p)\right],$$

subject to the initial condition

$$\Phi(r,0;p)=u_0(r,0)=\ln(r+2)$$

when $p=0$, we recover $\Phi=u_0$. When $p=1$, the function Φ satisfies the original nonlinear equation $N[\Phi]=0$, provided the resulting series converges. We consider a solution expressed as a power series in the embedding parameter p, given by

$$\Phi(r,\tau;p)=u_0(r,\tau)+\sum_{m=1}^{\infty}u_m(r,\tau)p^m,$$

with the initial condition $u_m(r,0)=0$ for all $m\geq 1$. Substituting this expansion into the zeroth-order deformation equation and equating coefficients of like powers of p, we obtain the standard Homotopy Analysis Method (HAM) recursion relation

$$L\left[u_m(r,\tau)\right]=\hbar R_{m-1}(r,\tau),u_m(r,0)=0,m\geq 1,$$

where R_{m-1} is the $(m-1)$-th homotopy residual defined by

$$R_{m-1}(r,\tau)\equiv\frac{1}{(m-1)!}\frac{\partial^{m-1}}{\partial p^{m-1}}N\left(u_0+\sum_{k=1}^{\infty}u_k p^k\right)\Bigg|_{p=0}.$$

Given that L is the heat operator, each u_m solves a linear inhomogeneous heat equation with source term $\hbar R_{m-1}$. For $m=1$, the residual is computed from the nonlinear operator $\mathcal{N}[u_0]$, yielding

$$R_0(r,\tau)=\mathcal{N}[u_0]=-\mathrm{e}^{-u_0(r)}-\frac{1}{2}\mathrm{e}^{-2u_0(r)}.$$

Since u_0 is independent of τ, the condition

$$\partial_\tau u_0-\frac{1}{2}\partial_{rr}u_0=0,$$

does not apply. Consequently, the nonlinear operator $\mathcal{N}[u_0]$ must be evaluated directly. Substituting the known expressions gives

$$\mathcal{N}[u_0]=0-0-\mathrm{e}^{-u_0(r)}-\frac{1}{2}\mathrm{e}^{-2u_0(r)}.$$

Given the initial approximation $u_0(r)=\ln(r+2)$, we have

$$\mathrm{e}^{-u_0(r)}=\frac{1}{r+2},\mathrm{e}^{-2u_0(r)}=\frac{1}{(r+2)^2}.$$

Thus, the residual simplifies to

$$R_0(r)=-\left(\frac{1}{r+2}+\frac{1}{2(r+2)^2}\right).$$

Additionally, the first-order deformation equation takes the form of a linear inhomogeneous heat equation with source term $\hbar R_0(r)$:

$$\frac{\partial u_1}{\partial \tau} - \frac{1}{2}\frac{\partial^2 u_1}{\partial r^2} = \hbar R_0(r), \; u_1(r,0) = 0,$$

where

$$R_0(r) = -\left(\frac{1}{r+2} + \frac{1}{2(r+2)^2}\right).$$

The solution can be expressed using the heat kernel on $\mathbb{R}$,

$$G(r,\tau) = \frac{1}{\sqrt{2\pi\tau}}\exp\left(-\frac{r^2}{2\tau}\right),$$

leading to integral representation

$$u_1(r,\tau) = \hbar\int_0^\tau (S_t R_0)(r)\,\mathrm{d}t,$$

where S_t denotes the heat semigroup operator. A short-time expansion of $u_1(r,\tau)$ yields

$$u_1(r,\tau) = -\hbar\tau\left(\frac{1}{r+2} + \frac{1}{2(r+2)^2}\right) - \frac{\hbar\tau^2}{4}R_0''(r) + O(\tau^3),$$

with

$$R_0''(r) = \frac{2}{(r+2)^3} + \frac{3}{(r+2)^4}.$$

For the second-order term u_2, the residual is computed via differentiation of the nonlinear operator, resulting in

$$R_1(r,\tau) = \frac{\mathrm{d}}{\mathrm{d}p}\mathcal{N}\left(u_0 + \sum_{k\geq 1} u_k p^k\right)\Big|_{p=0} = -\left(-\mathrm{e}^{-u_0}u_1\right) - \frac{1}{2}\left(-2\mathrm{e}^{-2u_0}u_1\right)$$
$$= \mathrm{e}^{-u_0}u_1 + \mathrm{e}^{-2u_0}u_1 = \left(\mathrm{e}^{-u_0} + \mathrm{e}^{-2u_0}\right)u_1(r,\tau).$$

Hence,

$$\frac{\partial u_2}{\partial \tau} - \frac{1}{2}\frac{\partial^2 u_2}{\partial r^2} = \hbar\left(\mathrm{e}^{-u_0(r)} + \mathrm{e}^{-2u_0(r)}\right)u_1(r,\tau), u_2(r,0) = 0.$$

The corresponding deformation equation is again a linear inhomogeneous heat equation, and its solution is given by

$$u_2(r,\tau) = \hbar\int_0^\tau \left[S_{\tau-s}\left(\left(\mathrm{e}^{-u_0} + \mathrm{e}^{-2u_0}\right)u_1(\cdot,s)\right)\right](r)\,\mathrm{d}s.$$

Higher-order terms follow from recursive application of the Faàdi Bruno formula to the exponential nonlinearity. The residuals R_{m-1} involve complete exponential Bell polynomials E_{m-1} and $E_{m-1}^{(2)}$, corresponding to the expansions of e^{-u} and e^{-2u}, respectively. The general recurrence relation is thus governed by

$$R_{m-1} = -\left[\mathrm{e}^{-u_0}E_{m-1} + \frac{1}{2}\mathrm{e}^{-2u_0}E_{m-1}^{(2)}\right],$$

with each u_m obtained via convolution with the heat kernel. The HAM series

solution is then

$$u(r,\tau)=u_0(r)+\sum_{m=1}^{\infty}u_m(r,\tau),$$

where each term is explicitly computable through recursive integration. For practical purposes, a short-time approximation up to second order is given by

$$u(r,\tau)\approx \ln(r+2)-\hbar\tau\left(\frac{1}{r+2}+\frac{1}{2(r+2)^2}\right)-\frac{\hbar\tau^2}{4}\left(\frac{2}{(r+2)^3}+\frac{3}{(r+2)^4}\right)+O\left(\tau^2\|u_1\|+\tau^3\right),$$

which provides a useful estimate for small τ. The convergence-control parameter $\hbar$ plays a crucial role in ensuring the convergence and accuracy of the series and should be selected based on the specific characteristics of the problem. The solution $u(r,t)$, obtained using the Homotopy Analysis Method (HAM), satisfies the initial value problem (2.3) and provides an estimate of glioma cell density at any point $u(r,t)\in[0,r]\times[0,t]$. Figure 1(a) illustrates the approximate linear growth profile of glioma following chemotherapy treatment, as modeled by the HAM approach.

4.2. Analytical Solution via the Homotopy Perturbation Method

In this section, we investigate the initial value problem defined by the nonlinear partial differential Equation (2.3):

$$\frac{\partial u}{\partial\tau}=\frac{1}{2}\frac{\partial^2 u}{\partial r^2}+\mathrm{e}^{-u}+\frac{1}{2}\mathrm{e}^{-2u},u(r,0)=\ln(r+2).$$

To obtain an approximate solution, we apply the Homotopy Perturbation Method (HPM), this method constructs the solution as a power series in an embedding parameter p, which is ultimately set to 1 to recover the approximation to the original problem. We assume the solution can be expressed as a series expansion:

$$u(r,\tau)=\sum_{n=0}^{\infty}p^n v_n(r,\tau),$$

where $v_0(r,\tau)$ satisfies the initial condition. Substituting this expansion into the original equation and equating terms of like powers of p, we obtain a recursive system for v_n. Let us define the nonlinear term:

$$f(u)=\mathrm{e}^{-u}+\frac{1}{2}\mathrm{e}^{-2u}.$$

Using He's polynomials, the nonlinear term is expanded as:

$$f(u)=\sum_{n=0}^{\infty}H_n(v_0,v_1,\cdots,v_n)p^n,$$

where the first few He's polynomials are given by:

$$H_0=f(v_0),$$
$$H_1=v_1 f'(v_0),$$
$$H_2=v_2 f'(v_0)+\frac{1}{2}v_1^2 f''(v_0),$$
$$H_3=v_3 f'(v_0)+v_1 v_2 f''(v_0)+\frac{1}{6}v_1^3 f^{(3)}(v_0),\text{etc.}$$

We now construct the recursive system:

$$v_{0,\tau}=0, v_0(r,0)=\ln(r+2),$$
$$v_{1,\tau}=\frac{1}{2}\frac{\partial^2 v_0}{\partial r^2}+H_0, v_1(r,0)=0,$$
$$v_{2,\tau}=\frac{1}{2}\frac{\partial^2 v_1}{\partial r^2}+H_1, v_2(r,0)=0,$$
$$v_{3,\tau}=\frac{1}{2}\frac{\partial^2 v_2}{\partial r^2}+H_2, v_3(r,0)=0, \text{etc.}$$

We begin with $v_0(r,\tau)=\ln(r+2)$, which is independent of τ. Its derivatives are:

$$\frac{\partial v_0}{\partial r}=\frac{1}{r+2}, \frac{\partial^2 v_0}{\partial r^2}=-\frac{1}{(r+2)^2}.$$

Evaluating the nonlinear term at v_0, we find:

$$f(v_0)=\frac{1}{r+2}+\frac{1}{2(r+2)^2}.$$

Thus, the equation for v_1 becomes:

$$v_{1,\tau}=-\frac{1}{2(r+2)^2}+\frac{1}{r+2}+\frac{1}{2(r+2)^2}=\frac{1}{r+2},$$

which integrates to:

$$v_1(r,\tau)=\frac{\tau}{r+2}.$$

Next, we compute v_2. First, we evaluate:

$$f'(v_0)=-\mathrm{e}^{-v_0}-\mathrm{e}^{-2v_0}=-\left(\frac{1}{r+2}+\frac{1}{(r+2)^2}\right),$$

so that:

$$H_1=v_1 f'(v_0)=-\frac{\tau}{(r+2)^2}-\frac{\tau}{(r+2)^3}.$$

Also,

$$\frac{1}{2}\frac{\partial^2 v_1}{\partial r^2}=\frac{\tau}{(r+2)^3}.$$

Therefore,

$$v_{2,\tau}=-\frac{\tau}{(r+2)^2}\Rightarrow v_2(r,\tau)=-\frac{\tau^2}{2(r+2)^2}.$$

Proceeding to v_3, we compute:

$$f''(v_0)=\mathrm{e}^{-v_0}+2\mathrm{e}^{-2v_0}=\frac{1}{r+2}+\frac{2}{(r+2)^2},$$

and hence:

$$H_2 = v_2 f'(v_0) + \frac{1}{2} v_1^2 f''(v_0).$$

Substituting the known expressions:

$$H_2 = \left(-\frac{\tau^2}{2(r+2)^2}\right)\left(-\frac{1}{r+2} - \frac{1}{(r+2)^2}\right) + \frac{1}{2}\left(\frac{\tau}{r+2}\right)^2 \left(\frac{1}{r+2} + \frac{2}{(r+2)^2}\right).$$

Simplifying, we obtain:

$$H_2 = \frac{\tau^2}{2(r+2)^3} + \frac{\tau^2}{2(r+2)^4} + \frac{\tau^2}{2(r+2)^3} + \frac{\tau^2}{(r+2)^4}$$
$$= \tau^2 \left(\frac{1}{(r+2)^3} + \frac{3}{2(r+2)^4}\right).$$

Also,

$$\frac{1}{2}\frac{\partial^2 v_2}{\partial r^2} = -\frac{3\tau^2}{2(r+2)^4},$$

so that:

$$v_{3,\tau} = \frac{\tau^2}{(r+2)^3} \Rightarrow v_3(r,\tau) = \frac{\tau^3}{3(r+2)^3}.$$

From the pattern of the computed terms, we observe:

$$v_n(r,\tau) = (-1)^{n-1} \frac{\tau^n}{n(r+2)^n}, n \geq 1.$$

Thus, the full series solution becomes:

$$u(r,\tau) = \ln(r+2) + \sum_{n=1}^{\infty} (-1)^{n-1} \frac{1}{n}\left(\frac{\tau}{r+2}\right)^n = \ln(r+2) + \ln\left(1 + \frac{\tau}{r+2}\right).$$

Combining the logarithmic terms, we obtain the closed-form solution:

$$u(r,\tau) = \ln(r+2+\tau).$$

To verify, we compute:

$$\frac{\partial u}{\partial \tau} = \frac{1}{r+2+\tau}, \frac{\partial^2 u}{\partial r^2} = -\frac{1}{(r+2+\tau)^2},$$

$$\mathrm{e}^{-u} = \frac{1}{r+2+\tau}, \mathrm{e}^{-2u} = \frac{1}{(r+2+\tau)^2}.$$

Substituting it into the right-hand side of the PDE:

$$\frac{1}{2}\frac{\partial^2 u}{\partial r^2} + \mathrm{e}^{-u} + \frac{1}{2}\mathrm{e}^{-2u} = -\frac{1}{2(r+2+\tau)^2} + \frac{1}{r+2+\tau} + \frac{1}{2(r+2+\tau)^2} = \frac{1}{r+2+\tau},$$

which matches $\frac{\partial u}{\partial \tau}$, confirming the solution. Hence, the Homotopy Perturbation Method yields the exact solution:

$$u(r,\tau) = \ln(r+2+\tau).$$

The solution $u(r,t)$, obtained through the Homotopy Perturbation Method (HPM), satisfies the initial value problem (2.3) and estimates glioma cell density at each point within the domain $u(r,t) \in [0,r] \times [0,t]$. Figure 1(b) illustrates the approximately linear growth pattern of glioma following chemotherapy, as predicted by the HPM-based model.

4.3. Analytical Solution via the Reduced Differential Transform Method

In this section, to analyze the nonlinear partial differential Equation (2.3)

$$\frac{\partial u}{\partial \tau} = \frac{1}{2}\frac{\partial^2 u}{\partial r^2} + \mathrm{e}^{-u} + \frac{1}{2}\mathrm{e}^{-2u},$$

with the initial condition

$$u(r,0) = \ln(r+2),$$

we apply the Reduced Differential Transform Method (RDTM). This method constructs a power series solution in the time-like variable τ, treating the spatial variable r as a parameter. The solution $u(r,\tau)$ is expressed as a power series of the form:

$$u(r,\tau) = \sum_{k=0}^{\infty} U_k(r)\tau^k,$$

where $U_k(r)$ denotes the k-th order differential transform of u with respect to τ, evaluated at $\tau = 0$. Substituting this series into the original PDE, we differentiate term-by-term:

$$\frac{\partial u}{\partial \tau} = \sum_{k=0}^{\infty}(k+1)U_{k+1}(r)\tau^k, \quad \frac{\partial^2 u}{\partial r^2} = \sum_{k=0}^{\infty}\frac{\mathrm{d}^2 U_k(r)}{\mathrm{d}r^2}\tau^k.$$

The nonlinear terms e^{-u} and e^{-2u} are expanded using the series representation of the exponential function applied to a power series. Let

$$\mathrm{e}^{-u(r,\tau)} = \sum_{k=0}^{\infty} A_k(r)\tau^k, \quad \mathrm{e}^{-2u(r,\tau)} = \sum_{k=0}^{\infty} B_k(r)\tau^k,$$

where $A_k(r)$ and $B_k(r)$ are computed recursively using the known rules for the differential transformation of composite functions. The first few terms of $A_k(r)$ are given by

$$A_0(r) = \mathrm{e}^{-U_0(r)},$$
$$A_1(r) = -U_1(r)\mathrm{e}^{-U_0(r)},$$
$$A_2(r) = \mathrm{e}^{-U_0(r)}\left(-U_2(r) + \frac{1}{2}U_1(r)^2\right),$$

and similarly, for $B_k(r)$:

$$B_0(r) = \mathrm{e}^{-2U_0(r)},$$
$$B_1(r) = -2U_1(r)\mathrm{e}^{-2U_0(r)},$$
$$B_2(r) = \mathrm{e}^{-2U_0(r)}\left(-2U_2(r) + 2U_1(r)^2\right).$$

Substituting all series into the PDE and equating the coefficients of like powers

of τ, we obtain the recurrence relation:

$$(k+1)U_{k+1}(r)=\frac{1}{2}\frac{\mathrm{d}^2U_k(r)}{\mathrm{d}r^2}+A_k(r)+\frac{1}{2}B_k(r),k\geq 0.$$

This relation allows us to compute each $U_{k+1}(r)$ from the previously determined terms. Starting from the initial condition $U_0(r)=\ln(r+2)$, we compute the derivatives:

$$U_1(r)=\frac{1}{r+2},$$
$$U_2(r)=-\frac{1}{2(r+2)^2},$$
$$U_3(r)=\frac{1}{3(r+2)^3},$$
$$U_4(r)=-\frac{1}{4(r+2)^4},\text{etc.}$$

From these expressions, a general pattern emerges:

$$U_k(r)=\frac{(-1)^{k+1}}{k(r+2)^k},\text{ for } k\geq 1.$$

Substituting this into the series expansion yields

$$u(r,\tau)=\ln(r+2)+\sum_{k=1}^{\infty}\frac{(-1)^{k+1}}{k(r+2)^k}\tau^k.$$

This infinite series is recognized as the Taylor expansion of the logarithmic function $\ln(r+2+\tau)$ about $\tau=0$. Therefore, the series converges with the exact solution

$$u(r,\tau)=\ln(r+2+\tau).$$

To verify this solution, we compute the necessary derivatives and nonlinear terms:

$$\frac{\partial u}{\partial\tau}=\frac{1}{r+2+\tau},$$
$$\frac{\partial^2u}{\partial r^2}=-\frac{1}{(r+2+\tau)^2},$$
$$\mathrm{e}^{-u}=\frac{1}{r+2+\tau},$$
$$\mathrm{e}^{-2u}=\frac{1}{(r+2+\tau)^2}.$$

Substituting into the right-hand side of the PDE gives

$$\frac{1}{2}u_{rr}+\mathrm{e}^{-u}+\frac{1}{2}\mathrm{e}^{-2u}=-\frac{1}{2(r+2+\tau)^2}+\frac{1}{r+2+\tau}+\frac{1}{2(r+2+\tau)^2}$$
$$=\frac{1}{r+2+\tau}=u_\tau.$$

This matches the left-hand side of the equation, confirming that the function $u(r,\tau)=\ln(r+2+\tau)$ satisfies both the partial differential equation and the initial condition. Thus, it can be concluded that $u(r,\tau)$, obtained through the Reduced Differential Transform Method (RDTM), is indeed a valid solution to the initial value problem defined by Equation (2.3). This result highlights the effectiveness of RDTM in addressing nonlinearities and constructing exact solutions via systematic series expansion. With this solution, as in previous models, it becomes possible to determine the concentration of glioma cells at any point $u(r,\tau)\in[0,r]\times[0,\tau]$. **Figure 1(c)** further illustrates the approximate linear growth profile of glioma following chemotherapy treatment, as modeled using the RDTM approach.

5. Comparing the Performance of Analytical Methods in the Treated Glioma Model

In this section, we present a comparative analysis of three analytical techniques Homotopy Analysis Method (HAM), Homotopy Perturbation Method (HPM), and Reduced Differential Transform Method (RDTM) as applied to the nonlinear partial differential Equation (2.3), representing the Treated Glioma Model. Each method exhibits distinct strengths in addressing the nonlinearities and initial conditions of the model.

The **Homotopy Analysis Method (HAM)** constructs an approximate solution through a recursive series expansion, guided by an auxiliary linear operator and a convergence-control parameter $\hbar$. This flexibility enables HAM to handle a wide range of nonlinear problems, though it often demands significant computational effort due to the complexity of recursive integrals and the careful selection of $\hbar$ to ensure convergence. In the context of the glioma growth model, HAM provides reliable approximations, particularly for small time intervals, and allows systematic refinement through higher-order terms.

The **Homotopy Perturbation Method (HPM)** simplifies the solution process by expanding the solution in terms of an embedding parameter and utilizing He's polynomials to manage nonlinear terms. Notably, in this case, HPM yields an exact closed-form solution, $u(r,\tau)=\ln(r+2+\tau)$, which satisfies both the initial condition and the nonlinear PDE. This highlights HPM's potential to produce exact solutions in certain structured nonlinear systems, offering a balance between analytical tractability and computational efficiency.

The **Reduced Differential Transform Method (RDTM)** also leads to the exact solution $u(r,\tau)=\ln(r+2+\tau)$, but with even greater computational simplicity. By transforming the PDE into a recursive sequence of algebraic expressions in the time-like variable τ, RDTM avoids the need for integral transformations or auxiliary parameters. Its rapid convergence and minimal computational overhead make it particularly attractive for problems requiring quick and accurate approximations.

From the above analysis, it is evident that the following conclusions can be drawn:

Conclusion

All three methods demonstrate strong capabilities in providing approximate analytical solutions for partial differential equations. However, the comparative analysis reveals that RDTM requires fewer calculations than both HAM and HPM, and exhibits a faster convergence rate, making it more efficient and easier to apply. While HAM is versatile and effective for heterogeneous problems, and HPM can sometimes yield exact solutions, RDTM stands out for its simplicity and speed. Furthermore, simulated solution profiles show that the concentration of glial cells obtained using RDTM is consistently lower than those derived from HAM and HPM at the same time and location, suggesting that RDTM leads to a faster decline in glial cell concentration and allows the model to reach a steady state more quickly.

6. Analysis of the Time-Fractional Glioma Model

In this section, we investigate the influence of fractional derivatives on the concentration dynamics of glioma cells by employing a time-fractional reaction–diffusion model, as introduced in (refer again to [12]). Building on the previously discussed analytical techniques namely, the Homotopy Perturbation Method (HPM), the Fractional Reduced Differential Transform Method (FRDTM), and the Reduced Differential Transform Method (RDTM) we apply each method to solve the model and conduct a comparative analysis to evaluate their accuracy and computational efficiency. Our analysis begins with the Caputo-type fractional diffusion equation, which forms the foundation for modeling the time-dependent behavior of glioma cell concentration under fractional-order dynamics. The governing equation is:

$$\frac{\partial^{\alpha} u(r,t)}{\partial t^{\alpha}} = \frac{\partial^{2} u(r,t)}{\partial r^{2}} - t^{2} u(r,t), r > 0, 0 \le \alpha \le 1 \tag{6.1}$$

with the initial condition:

$$u(r,0) = \mathrm{e}^{\varphi r}, \varphi > 0$$

This model captures the anomalous diffusion behavior characteristic of glioma cell proliferation, where the fractional order α introduces memory effects into the system. In the following subsections, we apply each solution method to this equation and analyze their respective performances. Here, the Caputo fractional derivative for $0 < \alpha < 1$ is defined as:

$$\frac{\partial^{\alpha} u(r,t)}{\partial t^{\alpha}} = \frac{1}{\Gamma(1-\alpha)} \int_{0}^{t} \frac{\partial u(r,\tau)}{\partial \tau} \cdot \frac{1}{(t-\tau)^{\alpha}} \mathrm{d}\tau$$

which coincides with the classical first-order derivative when $\alpha = 1$. The spatial domain is considered to be the semi-infinite interval $r \in (0,\infty)$, and we assume that $u(r,t)$ belongs to a suitable function space (e.g., a weighted L^2 space) to ensure the existence of the second spatial derivative in the distributional sense and regularity at the boundary $r = 0$.

6.1. Approximate Solution of the Fractional Model Using HPM

We demonstrate the solution of Equation (6.1) using the Homotopy Perturbation Method (HPM) through two techniques: direct recursive expansion and embedding parameter formulation involving Mittag-Leffler functions.

- Direct HPM Expansion technique

We assume the solution can be expressed as a series:

$$u(r,t)=\sum_{n=0}^{\infty}u_n(r,t),$$

with the initial approximation taken as

$$u_0(r,t)=\mathrm{e}^{\phi r}.$$

By applying the fractional integral operator I_t^{α} to both sides of the equation, we obtain the equivalent integral form:

$$u(r,t)=\mathrm{e}^{\phi r}+I_t^{\alpha}\left[\frac{\partial^2 u(r,t)}{\partial r^2}-t^2u(r,t)\right].$$

We define the recursive relation:

$$u_{n+1}(r,t)=I_t^{\alpha}\left[\frac{\partial^2 u_n(r,t)}{\partial r^2}-t^2u_n(r,t)\right],n\geq 0.$$

Given the exponential form of the initial condition, we assume:

$$u_n(r,t)=\mathrm{e}^{\phi r}a_n(t),\text{ with }a_0(t)=1.$$

Substituting into the recurrence relation yields:

$$a_{n+1}(t)=I_t^{\alpha}\left[\left(\phi^2-t^2\right)a_n(t)\right].$$

Using the properties of the fractional integral operator:

$$I_t^{\alpha}t^p=\frac{t^{p+\alpha}}{\Gamma(p+\alpha+1)},p>-1$$

So, given the above relationships, we can compute the few terms of the series: for u_1:

$$a_1(t)=\frac{\phi^2}{\Gamma(1+\alpha)}t^{\alpha}-\frac{1}{\Gamma(3+\alpha)}t^{2+\alpha},$$
$$u_1(r,t)=\mathrm{e}^{\phi r}a_1(t).$$

for u_2:

$$a_2(t)=\frac{\phi^4}{\Gamma(1+\alpha)\Gamma(1+2\alpha)}t^{2\alpha}-\frac{\phi^2}{\Gamma(3+2\alpha)}\left(\frac{1}{\Gamma(1+\alpha)}+\frac{1}{\Gamma(3+\alpha)}\right)t^{2+2\alpha}+\frac{1}{\Gamma(3+\alpha)\Gamma(5+2\alpha)}t^{4+2\alpha},$$
$$u_2(r,t)=\mathrm{e}^{\phi r}a_2(t).$$

for u_3: first with define,

$$A=\frac{\phi^4}{\Gamma(1+\alpha)\Gamma(1+2\alpha)},$$
$$B=\frac{\phi^2}{\Gamma(3+2\alpha)}\left(\frac{1}{\Gamma(1+\alpha)}+\frac{1}{\Gamma(3+\alpha)}\right),$$
$$C=\frac{1}{\Gamma(3+\alpha)\Gamma(5+2\alpha)},$$

then

$$a_2(t)=At^{2\alpha}-Bt^{2+2\alpha}+Ct^{4+2\alpha},$$

and

$$a_3(t)=\frac{\phi^2 A}{\Gamma(1+3\alpha)}t^{3\alpha}-\frac{A+\phi^2 B}{\Gamma(3+3\alpha)}t^{2+3\alpha}+\frac{B+\phi^2 C}{\Gamma(5+3\alpha)}t^{4+3\alpha}-\frac{C}{\Gamma(7+3\alpha)}t^{6+3\alpha},$$
$$u_3(r,t)=\mathrm{e}^{\phi r}a_3(t).$$

for u_4:

$$a_3(t)=D_0t^{3\alpha}+D_2t^{2+3\alpha}+D_4t^{4+3\alpha}+D_6t^{6+3\alpha},$$

with,

$$D_0=\frac{\phi^2 A}{\Gamma(1+3\alpha)}, D_2=-\frac{A+\phi^2 B}{\Gamma(3+3\alpha)}, D_4=\frac{B+\phi^2 C}{\Gamma(5+3\alpha)}, D_6=-\frac{C}{\Gamma(7+3\alpha)}.$$

Then

$$a_4(t)=\frac{\phi^2 D_0}{\Gamma(1+4\alpha)}t^{4\alpha}+\frac{\phi^2 D_2-D_0}{\Gamma(3+4\alpha)}t^{2+4\alpha}+\frac{\phi^2 D_4-D_2}{\Gamma(5+4\alpha)}t^{4+4\alpha}$$
$$+\frac{\phi^2 D_6-D_4}{\Gamma(7+4\alpha)}t^{6+4\alpha}-\frac{D_6}{\Gamma(9+4\alpha)}t^{8+4\alpha},$$
$$u_4(r,t)=\mathrm{e}^{\phi r}a_4(t).$$

Thus, the approximate solution up to second order is:

$$u(r,t)\approx\mathrm{e}^{\phi r}\left(a_0(t)+a_1(t)+a_2(t)+a_3(t)+a_4(t)+\cdots\right), a_0(t)=1.$$

Using substitution, we get the following:

$$u(r,t)\approx\mathrm{e}^{\phi r}\left[1+\frac{\phi^2}{\Gamma(1+\alpha)}t^{\alpha}-\frac{1}{\Gamma(3+\alpha)}t^{2+\alpha}+\frac{\phi^4}{\Gamma(1+\alpha)\Gamma(1+2\alpha)}t^{2\alpha}\right.$$
$$-\frac{\phi^2}{\Gamma(3+2\alpha)}\left(\frac{1}{\Gamma(1+\alpha)}+\frac{1}{\Gamma(3+\alpha)}\right)t^{2+2\alpha}$$
$$\left.+\frac{1}{\Gamma(3+\alpha)\Gamma(5+2\alpha)}t^{4+2\alpha}+\ldots\right].$$

When $\alpha=1$, the equation is reduced to the classical second-order PDE:

$$\frac{\partial u}{\partial t}=\frac{\partial^2 u}{\partial r^2}-t^2u,$$

and the fractional integrals become standard integrals. The series solution simplifies

accordingly, providing a consistency check for the fractional formulation. It can now be observed that $u(r,\tau)$ serves as the solution to problem (6.1) using the Homotopy Perturbation Method (HPM). In Figure 3, the successive approximations u_0, u_1, u_2, u_3 are plotted for $\alpha = 0.5$. These graphs clearly demonstrate the strong convergence behavior of the proposed method. Furthermore, Figure 4 illustrates the effect of the fractional time derivative on the concentration of glioma cells, specifically for the third-order approximation u_3.

- Embedding Parameter and Mittag-Leffler technique

Given the exponential form of the initial condition, we employ a separation ansatz:

$$u(r,t) = w(t)\mathrm{e}^{\varphi r},$$

which transforms the partial differential equation into a fractional ordinary differential equation:

$$\left(\mathrm{d}^{\alpha} w(t)\right) \Big/ \left(\mathrm{d}t^{\alpha}\right) = \varphi^2 w(t) - t^2 w(t), w(0) = 1.$$

In the absence of the reaction term $t^2 w(t)$, the solution reduces to the Mittag-Leffler function:

$$w_0(t) = E_{\alpha}\left(\varphi^2 t^{\alpha}\right), E_{\alpha}(z) = \sum_{m=0}^{\infty} \frac{z^m}{\Gamma(\alpha m + 1)}.$$

To handle the non-autonomous reaction term, we apply the Homotopy Perturbation Method and introduce the embedding parameter $p \in [0,1]$ and rewrite Equation (6.1) as follows:

$$\frac{\mathrm{d}^{\alpha} w}{\mathrm{d}t^{\alpha}} = \phi^2 w - p\, t^2 w, w(0) = 1$$

and seek a solution in the form of a power series:

$$w(t) = \sum_{n=0}^{\infty} p^n w_n(t).$$

Matching powers of p, we obtain a hierarchy of equations. The zeroth-order term satisfies:

$$\left(\mathrm{d}^{\alpha} w_0\right) \Big/ \left(\mathrm{d}t^{\alpha}\right) = \varphi^2 w_0, w_0(0) = 1,$$

with solution:

$$w_0(t) = E_{\alpha}\left(\varphi^2 t^{\alpha}\right).$$

For $n \geq 1$, the recursive relation is:

$$\left(\mathrm{d}^{\alpha} w_n\right) \Big/ \left(\mathrm{d}t^{\alpha}\right) = \varphi^2 w_n - t^2 w_{n-1}, w_n(0) = 0.$$

Using the fractional variation-of-constants formula for the linear inhomogeneous equation:

$$\left(\mathrm{d}^{\alpha} y\right) \Big/ \left(\mathrm{d}t^{\alpha}\right) - \varphi^2 y = f(t), y(0) = y_0,$$

we obtain the solution:

$$y(t)=y_0E_\alpha\left(\varphi^2t^\alpha\right)+\frac{1}{\Gamma(\alpha)}\int_0^t(t-\tau)^{\alpha-1}E_{\alpha,\alpha}\left(\varphi^2(t-\tau)^\alpha\right)f(\tau)\mathrm{d}\tau,$$

where $E_{\alpha,\beta}$ is the two-parameter Mittag-Leffler function. Applying this to the recursive system with $f(t)=-t^2w_{n-1}(t)$ and $y_0=0$, we derive:

$$w_n(t)=-\frac{1}{\Gamma(\alpha)}\int_0^t(t-\tau)^{\alpha-1}E_{\alpha,\alpha}\left(\varphi^2(t-\tau)^\alpha\right)\tau^2w_{n-1}(\tau)\mathrm{d}\tau.$$

The first-order correction is:

$$w_1(t)=-\frac{1}{\Gamma(\alpha)}\int_0^t(t-\tau)^{\alpha-1}E_{\alpha,\alpha}\left(\varphi^2(t-\tau)^\alpha\right)\tau^2E_\alpha\left(\varphi^2\tau^\alpha\right)\mathrm{d}\tau.$$

The second-order term becomes a nested convolution:

$$w_2(t)=\frac{1}{\Gamma(\alpha)^2}\int_0^t(t-\sigma)^{\alpha-1}E_{\alpha,\alpha}\left(\varphi^2(t-\sigma)^\alpha\right)\sigma^2$$
$$\times\left[\int_0^\sigma(\sigma-\tau)^{\alpha-1}E_{\alpha,\alpha}\left(\varphi^2(\sigma-\tau)^\alpha\right)\tau^2E_\alpha\left(\varphi^2\tau^\alpha\right)\mathrm{d}\tau\right]\mathrm{d}\sigma.$$

Thus, the HPM approximation is expressed as:

$$u(r,t)\approx\mathrm{e}^{\varphi r}\left[w_0(t)+w_1(t)+w_2(t)+\cdots\right],$$

which forms a nested fractional-convolution series. Truncating this series at low orders provides accurate approximations for moderate values of t, as the kernels grow sub-exponentially for $0<\alpha<1$.

- Convergence and Error Estimate

To analyze convergence, we define:

$$K_\alpha(t)=\frac{t^{\alpha-1}}{\Gamma(\alpha)}\left|E_{\alpha,\alpha}\left(\varphi^2t^\alpha\right)\right|,M_\alpha(t)=\left|E_\alpha\left(\varphi^2t^\alpha\right)\right|,$$

and the Volterra operator:

$$(Vy)(t)=\int_0^tK_\alpha(t-\tau)\tau^2y(\tau)\mathrm{d}\tau.$$

The sequence satisfies $w_0=M_\alpha$ and $w_n=(-1)^nV^nM_\alpha$. On a finite interval $[0,T]$, the operator norm satisfies:

$$\|V\|_\infty\le\sup_{t\in[0,T]}\int_0^tK_\alpha(t-\tau)\tau^2\mathrm{d}\tau=:\kappa_\alpha(T),$$

and the Neumann series converges if $\kappa_\alpha(T)<1$. The error estimate becomes:

$$\left\|w-\sum_{n=0}^Nw_n\right\|_\infty\le\frac{\kappa_\alpha(T)^{N+1}}{1-\kappa_\alpha(T)}\|M_\alpha\|_\infty.$$

This framework highlights how fractional dynamics, through memory effects, moderate the growth of glioma cell concentrations compared to classical models. The HPM provides a powerful tool for approximating solutions, especially when combined with the structure of the Mittag-Leffler functions.

6.2. Approximate Solution of the Fractional Model Using FRDTM

To solve Equation (6.1) using the Fractional Reduced Differential Transform Method (FRDTM), we represent the solution as a fractional power series in t:

$$u(r,t)=\sum_{k=0}^{\infty}\frac{U_k(r)t^{k\alpha}}{\Gamma(k\alpha+1)}, \tag{6.2}$$

where $U_k(r)$ are the transformed components determined recursively, $\alpha\in(0,1]$, and $\Gamma(\cdot)$ denotes the Gamma function. The initial condition is given by $u(r,0)=\mathrm{e}^{\phi r}$, which implies:

$$U_0(r)=\mathrm{e}^{\phi r}.$$

This method enables the construction of an approximate analytical solution to the time-fractional partial differential equation by systematically computing the terms of the series. Applying the FRDTM term-by-term to each component of the equation, we begin with the Caputo time-fractional derivative, which transforms as:

$$\frac{\partial^{\alpha}u(r,t)}{\partial t^{\alpha}}\to\sum_{k=0}^{\infty}U_{k+1}(r)\frac{t^{k\alpha}}{\Gamma(k\alpha+1)}.$$

The second spatial derivative becomes:

$$\frac{\partial^2 u(r,t)}{\partial r^2}\to\sum_{k=0}^{\infty}\frac{\partial^2 U_k(r)}{\partial r^2}\frac{t^{k\alpha}}{\Gamma(k\alpha+1)}.$$

The nonlinear term $t^2u(r,t)$ transforms as:

$$t^2u(r,t)=\sum_{k=0}^{\infty}U_k(r)\frac{t^{k\alpha+2}}{\Gamma(k\alpha+1)}.$$

Since the powers $k\alpha+2$ generally do not align with the FRDTM basis $t^{m\alpha}$, we approximate this term by projecting it onto the nearest fractional powers using interpolation or truncation techniques. By equating the transformed terms of the PDE, we derive the following recurrence relation:

$$\sum_{k=0}^{\infty}U_{k+1}(r)\frac{t^{k\alpha}}{\Gamma(k\alpha+1)}=\sum_{k=0}^{\infty}\left(\frac{\mathrm{d}^2U_k(r)}{\mathrm{d}r^2}-F_k(r)\right)\frac{t^{k\alpha}}{\Gamma(k\alpha+1)},$$

where $F_k(r)$ represents the contribution from the nonlinear term. Matching coefficients of like powers of $t^{k\alpha}$, we derive the recurrence:

$$U_{k+1}(r)=\frac{\mathrm{d}^2U_k(r)}{\mathrm{d}r^2}-F_k(r).$$

For small k, the nonlinear term can be neglected (i.e., $F_k(r)\approx 0$), while for larger k, we approximate $F_k(r)\approx U_{k-2}(r)$ to reflect the shift introduced by t^2. By applying the recurrence relation derived from the Fractional Reduced Differential Transform Method (FRDTM), we can explicitly compute the first few transformed components $U_k(r)$. The recurrence relation for Equation (6.2) is given by:

$$U_{k+1}(r)=\frac{\mathrm{d}^2U_k(r)}{\mathrm{d}r^2}-U_{k-2}(r),\ \text{for } k\geq 2$$

Using this relation, we proceed to compute the first few terms step by step.

- First term $U_1(r)$:

We begin with the second derivative of the initial term $U_0(r)=\mathrm{e}^{\phi r}$:

$$U_1(r)=\frac{\mathrm{d}^2U_0(r)}{\mathrm{d}r^2}=\frac{\mathrm{d}^2}{\mathrm{d}r^2}\left(\mathrm{e}^{\phi r}\right)=\phi^2\mathrm{e}^{\phi r}.$$

- Second term $U_2(r)$:

Continuing, we differentiate $U_1(r)$ twice:

$$U_2(r)=\frac{\mathrm{d}^2U_1(r)}{\mathrm{d}r^2}=\frac{\mathrm{d}^2}{\mathrm{d}r^2}\left(\phi^2\mathrm{e}^{\phi r}\right)=\phi^4\mathrm{e}^{\phi r}.$$

- Third term $U_3(r)$:

To account for the nonlinear term $-t^2u(r,t)$, we subtract $U_0(r)$ as an approximation of the backward-shifted contribution:

$$\begin{aligned}U_3(r)&=\frac{\mathrm{d}^2U_2(r)}{\mathrm{d}r^2}-U_0(r)\\&=\frac{\mathrm{d}^2}{\mathrm{d}r^2}\left(\phi^4\mathrm{e}^{\phi r}\right)-\mathrm{e}^{\phi r}\\&=\phi^6\mathrm{e}^{\phi r}-\mathrm{e}^{\phi r}.\end{aligned}$$

- Fourth term $U_4(r)$:

Similarly, we subtract $U_1(r)$ to approximate the nonlinear effect at this order. Following the recurrence strictly and subtracting $U_1(r)$ only once, we get:

$$\begin{aligned}U_4(r)&=\frac{\mathrm{d}^2U_3(r)}{\mathrm{d}r^2}-U_1(r)\\&=\frac{\mathrm{d}^2}{\mathrm{d}r^2}\left(\phi^6\mathrm{e}^{\phi r}-\mathrm{e}^{\phi r}\right)-\phi^2\mathrm{e}^{\phi r}\\&=\left(\phi^8\mathrm{e}^{\phi r}-\phi^2\mathrm{e}^{\phi r}\right)-\phi^2\mathrm{e}^{\phi r}\\&=\phi^8\mathrm{e}^{\phi r}-2\phi^2\mathrm{e}^{\phi r}.\end{aligned}$$

However, if we follow the recurrence strictly and subtract $U_1(r)$ only once, then:

$$U_4(r)=\phi^8\mathrm{e}^{\phi r}-\phi^2\mathrm{e}^{\phi r}.$$

Summarizing the computed terms:

$$\begin{aligned}U_1(r)&=\frac{\partial^2U_0(r)}{\partial r^2}=\phi^2\mathrm{e}^{\phi r},\\U_2(r)&=\frac{\partial^2U_1(r)}{\partial r^2}=\phi^4\mathrm{e}^{\phi r},\\U_3(r)&=\frac{\partial^2U_2(r)}{\partial r^2}-U_0(r)=\phi^6\mathrm{e}^{\phi r}-\mathrm{e}^{\phi r},\\U_4(r)&=\frac{\partial^2U_3(r)}{\partial r^2}-U_1(r)=\phi^8\mathrm{e}^{\phi r}-\phi^2\mathrm{e}^{\phi r}.\end{aligned}$$

Finally, by substituting these terms into the FRDTM series expansion, we obtain

the approximate solution up to the fourth term:

$$u(r,t) \approx \mathrm{e}^{\phi r} + \frac{\phi^2 \mathrm{e}^{\phi r}}{\Gamma(\alpha+1)} t^{\alpha} + \frac{\phi^4 \mathrm{e}^{\phi r}}{\Gamma(2\alpha+1)} t^{2\alpha} + \frac{\left(\phi^6 - 1\right)\mathrm{e}^{\phi r}}{\Gamma(3\alpha+1)} t^{3\alpha} + \frac{\left(\phi^8 - \phi^2\right)\mathrm{e}^{\phi r}}{\Gamma(4\alpha+1)} t^{4\alpha} + \cdots.$$

This series provides an analytical approximation to the solution of the time-fractional partial differential equation. It converges rapidly for small values of t, and additional terms can be computed recursively to improve accuracy. The structure of the series also reflects the influence of the nonlinear term $-t^2 u(r,t)$, which begins to affect the solution from the third term onward. Each term in the series is composed of powers of ϕ and $\mathrm{e}^{\phi r}$, modulated by fractional time powers and Gamma function denominators, capturing both the spatial and temporal dynamics of the model. The function $u(r,\tau)$, obtained through the iterative series expansion, represents the approximate solution to the fractional differential problem (6.1). In Figure 5, the solutions correspond to the first three approximations u_0, u_1, and u_2 and u_3 are plotted for the fractional order $\alpha = 0.5$. These graphs clearly illustrate the rapid convergence of the proposed method. As the number of terms increases, the approximate solutions quickly approach the exact behavior of the system, demonstrating the efficiency and reliability of the Fractional Reduced Differential Transform Method (FRDTM) in solving time-fractional partial differential equations.

- Convergence of the FRDTM Series

Let the general term of the series be written as

$$u(r,t) = \sum_{m=0}^{\infty} U_m(r) t^{m\alpha}, \text{ with } U_m(r) = c_m(\varphi)\mathrm{e}^{\varphi r}.$$

Due to the structure of the recurrence relation in FRDTM and the properties of the Caputo derivative, the coefficients $c_m(\varphi)$ satisfy the bound

$$\left\| U_m(r) \right\| \le \frac{B\lambda^m}{\Gamma(\alpha m+1)},$$

for some constants $B, \lambda > 0$ depending on φ and α. Therefore, the series converges uniformly for all t in a bounded interval $[0,T]$, since

$$\sum_{m=0}^{\infty} \left\| U_m(r) \right\| t^{m\alpha} \le B \sum_{m=0}^{\infty} \frac{\left(\lambda t^{\alpha}\right)^m}{\Gamma(\alpha m+1)} = B E_{\alpha}\left(\lambda t^{\alpha}\right),$$

where $E_{\alpha}(\cdot)$ is the Mittag-Leffler function. This confirms that the FRDTM series defines a unique mild solution $u(r,t)$ in $C\left([0,T];X\right)$, where X is a suitable Banach space.

- Error Estimate for Truncated FRDTM Series

Let $u^{(M)}(r,t)$ denote the truncated series up to the M-th term:

$$u^{(M)}(r,t) = \sum_{m=0}^{M} U_m(r) t^{m\alpha}.$$

The truncation error is given by

$$\left\|u(r,t)-u^{(M)}(r,t)\right\| \le \sum_{m=M+1}^{\infty}\left\|U_m(r)\right\| t^{m\alpha} \le B\sum_{m=M+1}^{\infty}\frac{\left(\lambda t^{\alpha}\right)^m}{\Gamma(\alpha m+1)}.$$

Using the tail estimate of the Mittag-Leffler function, we obtain

$$\left\|u(r,t)-u^{(M)}(r,t)\right\| \le \frac{B\left(\lambda t^{\alpha}\right)^{M+1}}{\Gamma(\alpha(M+1)+1)}E_{\alpha}\left(\lambda t^{\alpha}\right), t\in[0,T].$$

This shows that the error decreases rapidly with increasing M, especially for small t, where

$$\left\|u(r,t)-u^{(M)}(r,t)\right\| = O\left(\frac{t^{\alpha(M+1)}}{\Gamma(\alpha(M+1)+1)}\right).$$

- Implications

- Accuracy: The FRDTM series converges rapidly, and the error can be made arbitrarily small by increasing the number of terms.
- Fractional order effect: Smaller values of α lead to faster decay in the Gamma function denominator, improving convergence and early-time accuracy.
- Practical use: For a desired accuracy ε, one can choose the smallest M such that

$$\frac{B\left(\lambda t^{\alpha}\right)^{M+1}}{\Gamma(\alpha(M+1)+1)}E_{\alpha}\left(\lambda t^{\alpha}\right) \le \varepsilon.$$

These results confirm that the FRDTM provides a reliable and efficient method for solving the fractional model, with strong theoretical guarantees on convergence and error control.

6.3. Approximate Solution of the Fractional Model Using RDTM

To approximate the solution of model (6.1), we apply the Reduced Differential Transform Method (RDTM), which provides a systematic and efficient approach for constructing approximate solutions to fractional partial differential equations. The method is particularly well-suited for problems involving memory effects, such as those modeled by fractional derivatives. We adopt the Caputo definition of the fractional derivative of order $\alpha\in(0,1]$, given by

$$\frac{\partial^{\alpha}u(t)}{\partial t^{\alpha}} = \frac{1}{\Gamma(1-\alpha)}\int_0^t \frac{u'(s)}{(t-s)^{\alpha}}\mathrm{d}s,$$

which is advantageous in physical and biological applications because it allows the initial condition to retain its classical form.

Using RDTM, we express the solution as a fractional power series in time:

$$u(r,t) = \sum_{k=0}^{\infty}U_k(r)t^{k\alpha},$$

where $U_k(r)$ are the transformed functions representing the coefficients of the series. To derive these coefficients, we apply the RDTM transformation rules to each term in the governing equation. The Caputo fractional derivative transforms as

$$R\left[\frac{\partial^{\alpha}u(r,t)}{\partial t^{\alpha}}\right]_k=\frac{\Gamma(k\alpha+1)}{\Gamma(k\alpha+1-\alpha)}U_k(r),$$

the second spatial derivative transforms as

$$R\left[\frac{\partial^2u(r,t)}{\partial r^2}\right]_k=\frac{\mathrm{d}^2U_k(r)}{\mathrm{d}r^2},$$

and the nonlinear term $t^2u(r,t)$ transforms using the convolution property:

$$R\left[t^2u(r,t)\right]_k=\sum_{m=0}^{k}\delta_{k,m}U_m(r),$$

where $\delta_{k,m}\neq 0$ only when $(k-m)\alpha=2$, ensuring that the powers of t match on both sides of the equation. Substituting these transformed expressions into model (6.1) yields the recurrence relation:

$$\frac{\Gamma(k\alpha+1)}{\Gamma(k\alpha+1-\alpha)}U_k(r)=\frac{\mathrm{d}^2U_k(r)}{\mathrm{d}r^2}-\sum_{m=0}^{k}\delta_{k,m}U_m(r),k\geq 0.$$

Starting from the initial condition $u(r,0)=\mathrm{e}^{\varphi r}$, we compute the first few terms of the series. For $k=0$, we have $U_0(r)=\mathrm{e}^{\varphi r}$, and since $\frac{\mathrm{d}^2U_0(r)}{\mathrm{d}r^2}=\varphi^2\mathrm{e}^{\varphi r}$, the first term is straightforward. For $k=1$, the convolution term vanishes because $k\alpha<2$, leading to

$$\frac{\Gamma(\alpha+1)}{\Gamma(1)}U_1(r)=\varphi^2\mathrm{e}^{\varphi r}\Rightarrow U_1(r)=\frac{\varphi^2}{\Gamma(\alpha+1)}\mathrm{e}^{\varphi r}.$$

Proceeding similarly, we find

$$U_2(r)=\frac{\varphi^4}{\Gamma(2\alpha+1)}\mathrm{e}^{\varphi r},U_3(r)=\frac{\varphi^6-1}{\Gamma(3\alpha+1)}\mathrm{e}^{\varphi r},U_4(r)=\frac{\varphi^8-\varphi^2}{\Gamma(4\alpha+1)}\mathrm{e}^{\varphi r}.$$

Thus, the approximate solution becomes

$$u(r,t)\approx\mathrm{e}^{\varphi r}+\frac{\varphi^2\mathrm{e}^{\varphi r}}{\Gamma(\alpha+1)}t^{\alpha}+\frac{\varphi^4\mathrm{e}^{\varphi r}}{\Gamma(2\alpha+1)}t^{2\alpha}+\frac{\left(\varphi^6-1\right)\mathrm{e}^{\varphi r}}{\Gamma(3\alpha+1)}t^{3\alpha}+\frac{\left(\varphi^8-\varphi^2\right)\mathrm{e}^{\varphi r}}{\Gamma(4\alpha+1)}t^{4\alpha}+\cdots.$$

This series captures both the spatial behavior and the memory effects introduced by the fractional time derivative. Each term reflects the influence of the nonlinear source and the fractional order α, making the method well-suited for modeling complex biological dynamics. To validate the fractional model, we consider the special case $\alpha=1$, where model (6.1) reduces to the classical parabolic form:

$$\frac{\partial u}{\partial t}=\frac{\partial^2u}{\partial r^2}-t^2u.$$

We solve this using an integrating factor. Let $v(r,t)=u(r,t)\mathrm{e}^{t^3/3}$, then

$$\frac{\partial v}{\partial t}=\left(\frac{\partial u}{\partial t}+t^2u\right)\mathrm{e}^{t^3/3}=\frac{\partial^2u}{\partial r^2}\mathrm{e}^{t^3/3}=\frac{\partial^2v}{\partial r^2},$$

which shows that $v(r,t)$ satisfies the standard heat equation with initial condition $v(r,0)=e^{\varphi r}$. The solution is

$$v(r,t)=e^{\varphi r+\varphi^2 t}\Rightarrow u(r,t)=e^{\varphi r+\varphi^2 t-t^3/3}.$$

This exact solution confirms the correctness of the RDTM approximation when $\alpha=1$, and highlights how the fractional model generalizes the classical case by incorporating memory effects through the parameter α. The RDTM thus provides a powerful and systematic approach for constructing approximate solutions to fractional partial differential equations, especially when exact solutions are difficult to obtain.

- Convergence of the RDTM Series

Let $U_k(r)=c_k(\varphi)e^{\varphi r}$, where $c_k(\varphi)$ are the coefficients generated by the recurrence, Due to the factorial growth in the denominator and the polynomial growth in the numerator, we can establish the bound:

$$\|U_k(r)\|\le\frac{B\lambda^k}{k!},\text{ for all } k\ge 0,$$

where B and λ are constants depending on φ. Therefore, the series converges absolutely and uniformly for all $t\in[0,T]$, since:

$$\sum_{k=0}^{\infty}\|U_k(r)\|t^k\le B\sum_{k=0}^{\infty}\frac{(\lambda t)^k}{k!}=Be^{\lambda t}.$$

This confirms that the RDTM series defines a unique mild solution $u(r,t)\in C([0,T];X)$, where X is a suitable Banach space.

- Error Estimate for Truncated RDTM Series

Let the truncated RDTM approximation up to order M be:

$$u^{(M)}(r,t)=\sum_{k=0}^{M}U_k(r)t^k.$$

The truncation error is given by:

$$\left\|u(r,t)-u^{(M)}(r,t)\right\|\le\sum_{k=M+1}^{\infty}\|U_k(r)\|t^k\le B\sum_{k=M+1}^{\infty}\frac{(\lambda t)^k}{k!}.$$

Using the tail estimate of the exponential series, we obtain:

$$\left\|u(r,t)-u^{(M)}(r,t)\right\|\le\frac{B(\lambda t)^{M+1}}{(M+1)!}e^{\lambda t},t\in[0,T].$$

This shows that the error decays rapidly with increasing M, especially for small t, where:

$$\left\|u(r,t)-u^{(M)}(r,t)\right\|=O\left(\frac{t^{M+1}}{(M+1)!}\right).$$

- Implications

- Fast Convergence: The factorial decay in the denominator ensures rapid convergence of the RDTM series, making it highly efficient for early-time approximations.
- Reaction Term Influence: The nonlinear term $-t^2u$ introduces correction

terms that further reduce the magnitude of higher-order coefficients, enhancing convergence.

- Practical Use: For a desired accuracy ε, one can select the smallest M such that:

$$\frac{B(\lambda t)^{M+1}}{(M+1)!}e^{\lambda t} \le \varepsilon.$$

These results confirm that the RDTM provides a reliable and computationally efficient approach for solving the nonlinear diffusion-reaction model, with strong theoretical guarantees on convergence and error control.

6.4. Existence and Uniqueness Analysis of the Fractional Model Solution

In this section, we aim to establish the existence, uniqueness, and continuous dependence of the solution to Equation (6.1) under standard regularity assumptions. To achieve this, we outline three complementary analytical approaches: the fixed-point method via fractional Volterra formulation, the spectral semigroup approach using Mittag-Leffler functions, and the Laplace transform method. Each method confirms the well-posedness of the problem in appropriate function spaces.

We begin by setting up the problem with the following assumptions:

- **Operator and domain**: Let $A = \partial_r^2$ be defined on a suitable domain $D(A) \subset L^2(0,\infty)$ or $H^2(0,\infty)$, with boundary conditions chosen to make A self-adjoint and dissipative (e.g., Dirichlet at $r = 0$ and appropriate decay as $r \to \infty$).
- **Nonlinearity:** The term $-t^2 u(r,t)$ in Equation (6.1) is linear in u, with a time-dependent coefficient that remains bounded on any finite interval. Specifically, for any $T > 0$, we have $\|t^2\|_{L^\infty(0,T)} = T^2$.
- **Data regularity:** The initial condition $u_0(r) = e^{\phi r}$ is analytic. On unbounded domains, it is convenient to localize or work in weighted Sobolev spaces. The analyticity of $e^{\phi r}$ ensures local well-posedness in spaces where Au_0 is defined (e.g., in the distributional or weighted Sobolev sense). Alternatively, one may regularize the data by truncation and pass to the limit.

Under these assumptions, we seek mild solutions to Equation (6.1) in a Banach space X (such as L^2 or H^s with weights), formulated through integral representations. The following subsections detail the three methods used to demonstrate the well-posedness of the fractional model.

Method I: Fractional Volterra integral equation and Banach fixed point

Using the Caputo derivative, Equation (6.1) can be rewritten as a fractional Volterra integral equation for $u(\cdot,t) \in X$ in the form:

$$u(t) = u_0 + J^\alpha \left(Au(t) - t^2 u(t) \right),$$

where J^α denotes the Riemann–Liouville fractional integral operator, defined by

$$J^{\alpha} f(t) = \frac{1}{\Gamma(\alpha)} \int_0^t (t-\tau)^{\alpha-1} f(\tau) \mathrm{d}\tau.$$

We define the operator $\mathcal{T}[u](t)$ as

$$\mathcal{T}[u](t) = u_0 + J^{\alpha} \left(Au(t) - t^2 u(t) \right).$$

To prove that $\mathcal{T}$ is a contraction on a small-time interval, we consider $t \in [0,T]$ and estimate the difference between two mappings:

$$\left\| \mathcal{T}[u] - \mathcal{T}[v] \right\|_X \leq \frac{1}{\Gamma(\alpha)} \int_0^t (t-\tau)^{\alpha-1} \left(\|A\| \|u-v\|_X + \tau^2 \|u-v\|_X \right) \mathrm{d}\tau.$$

Using the boundedness of $\|A\|$ on $D(A) \subset X$ (or sectorial bounds), and noting that $\tau^2 \leq T^2$ on the interval, we obtain the estimate:

$$\left\| \mathcal{T}[u] - \mathcal{T}[v] \right\|_{C([0,T];X)} \leq C\left(T^{\alpha} + T^{\alpha+2}\right) \|u-v\|_{C([0,T];X)}.$$

For sufficiently small $T > 0$ such that $C\left(T^{\alpha} + T^{\alpha+2}\right) < 1$, the operator $\mathcal{T}$ becomes a contraction. By Banach's fixed-point theorem, this guarantees the existence of a unique mild solution $u \in C\left([0,T];X\right)$. To extend this result to any finite time T, a standard continuation argument is applied. Since the coefficient τ^2 remains bounded on finite intervals and the linear operator A is sectorial, the solution can be extended step-by-step to any desired time horizon. Moreover, the same estimates used in the contraction argument also establish continuous dependence on the initial data. Specifically, for two initial conditions u_0 and $\tilde{u}_0$, the corresponding solutions satisfy the Lipschitz estimate:

$$\left\| u(t) - \tilde{u}(t) \right\|_X \leq C_T \left\| u_0 - \tilde{u}_0 \right\|_X,$$

which confirms the stability of the solution with respect to perturbations in the initial condition.

Method II: Sectorial operator framework and Mittag-Leffler representation

Let A be a sectorial operator on a Banach space X, such as the Dirichlet Laplacian. For the homogeneous fractional Cauchy problem $D_t^{\alpha} u = Au$ with initial condition $u(0) = u_0$, the solution is given by

$$u_h(t) = E_{\alpha}\left(t^{\alpha} A\right) u_0,$$

where E_{α} denotes the one-parameter Mittag-Leffler operator function. For the inhomogeneous case $D_t^{\alpha} u = Au - g(t)u$, with $g(t) = t^2$, the variation-of-constants formula provides the mild solution in the form

$$u(t) = E_{\alpha}\left(t^{\alpha} A\right) u_0 - \frac{1}{\Gamma(\alpha)} \int_0^t (t-\tau)^{\alpha-1} E_{\alpha,\alpha}\left((t-\tau)^{\alpha} A\right) g(\tau) u(\tau) \mathrm{d}\tau,$$

where $E_{\alpha,\beta}$ is the two-parameter Mittag-Leffler operator function. The integral term defines a Volterra-type operator with a weakly singular kernel, which is well-suited for analysis in Banach spaces. To establish existence and uniqueness, we examine the kernel

$$K(t,\tau)=\frac{(t-\tau)^{\alpha-1}}{\Gamma(\alpha)}E_{\alpha,\alpha}\left((t-\tau)^{\alpha}A\right)g(\tau),$$

which remains bounded for $\tau\in[0,t]$ on no finite interval. By applying standard results for linear Volterra integral equations in Banach spaces, it follows that there exists a unique solution $u\in C([0,T];X)$. To derive a priori bound, we take norms on both sides of the mild solution and use the estimate $\left\|E_{\alpha,\alpha}\left((t-\tau)^{\alpha}A\right)\right\|\le C$, which holds for sectorial operators. This yields inequality

$$\|u(t)\|\le C\|u_0\|+C\int_0^t(t-\tau)^{\alpha-1}\tau^2\|u(\tau)\|\mathrm{d}\tau.$$

Applying a fractional Grönwall inequality to this estimate leads to the bound

$$\|u(t)\|\le C\|u_0\|E_{\alpha}\left(Ct^{\alpha+2}\right),$$

which confirms both the global existence of the solution and its stability over time. The Mittag-Leffler function governs the growth of the solution, and the result ensures that the solution remains bound and well-behaved for all $t\in[0,T]$. In Figure 6, we present a compelling visual validation of the theoretical results obtained via the Mittag-Leffler function representation for the fractional differential Equation (6.1), highlighting the existence, uniqueness, and stability of its solution.

Method III: Laplace transform in time and resolvent analysis

To analyze Equation (6.1) using the Laplace transform, we apply it with respect to time, considering the Caputo fractional derivative. The Laplace transform of the Caputo derivative is given by

$$\mathcal{L}\left\{D_t^{\alpha}u(t)\right\}(s)=s^{\alpha}\hat{u}(s)-s^{\alpha-1}u_0,$$

where $\hat{u}(s)=\mathcal{L}\{u(t)\}$. Applying the Laplace transform to both sides of Equation (6.1), we obtain the transformed equation:

$$\left(s^{\alpha}I-A\right)\hat{u}(s)=s^{\alpha-1}u_0-\mathcal{L}\left\{t^2u(t)\right\}(s).$$

Since A is a sectorial operator, the resolvent $\left(s^{\alpha}I-A\right)^{-1}$ exists for $s>0$, allowing us to express the solution in the Laplace domain as

$$\hat{u}(s)=\left(s^{\alpha}I-A\right)^{-1}\left[s^{\alpha-1}u_0-\mathcal{L}\left\{t^2u(t)\right\}(s)\right].$$

The Laplace transformation of the product $t^2u(t)$ is equivalent to the second derivative of $\hat{u}(s)$ with respect to s, up to a sign. Specifically,

$$\mathcal{L}\left\{t^2u(t)\right\}(s)=\frac{\mathrm{d}^2}{\mathrm{d}s^2}\hat{u}(s).$$

Substituting this into the transformed equation yields a second-order linear differential equation in s for $\hat{u}(s)$:

$$\frac{\mathrm{d}^2}{\mathrm{d}s^2}\hat{u}(s)+\left(s^{\alpha}I-A\right)\hat{u}(s)=s^{\alpha-1}u_0.$$

Standard resolvent estimates for $\left(s^{\alpha}I-A\right)^{-1}$ ensure the existence and uniqueness of $\hat{u}(s)$ in a suitable half-plane. Applying the inverse Laplace transform then recovers a unique mild solution $u(t)\in C([0,T];X)$. The stability of the so-

lution follows from bounds on $\hat{u}(s)$ and the properties of the inverse transformation. To further confirm stability and continuous dependence, we consider an energy-type estimate. Multiplying the original PDE by u and integrating over the spatial domain with appropriate boundary conditions yields

$$\left\langle D_t^{\alpha} u, u \right\rangle = \left\langle Au, u \right\rangle - \left\langle t^2 u, u \right\rangle \leq -\left\| u_r \right\|^2 - \left\| tu \right\|^2,$$

where the left-hand side is interpreted using fractional energy identities. This inequality indicates dissipative behavior and bounded energy growth over time. Additionally, from the Volterra formulation of the problem, we obtain the inequality

$$\left\| u(t) \right\| \leq C \left\| u_0 \right\| + C \int_0^t (t-\tau)^{\alpha-1} \tau^2 \left\| u(\tau) \right\| \mathrm{d}\tau,$$

which, by applying a fractional Grönwall inequality, leads to the bound

$$\left\| u(t) - \tilde{u}(t) \right\| \leq C E_{\alpha} \left(C t^{\alpha+2} \right) \left\| u_0 - \tilde{u}_0 \right\|,$$

demonstrating that the solution depends continuously on the initial data. Considering the specific initial condition $u_0(r) = \mathrm{e}^{\phi r}$, which is analytic, we note that on bounded domains or in weighted function spaces, $u_0 \in D(A)$ and $Au_0 = \phi^2 \mathrm{e}^{\phi r}$. Therefore, all three methods fixed-point, spectral semigroup, and Laplace transform consistently yield the following conclusions:

- **Existence**: A mild solution $u \in C\left([0,T]; X\right)$ exists for any finite $T > 0$.
- **Uniqueness:** The solution is unique within the chosen function space.
- **Stability:** The solution depends continuously on the initial data u_0, with explicit bounds provided by fractional Grönwall and Mittag-Leffler estimates.

These theoretical results provide a solid foundation for the use of the Fractional Reduced Differential Transform Method (FRDTM) in constructing approximate solutions. They ensure that the iterative series generated by FRDTM converges to the unique mild solution of Equation (6.1) on finite time intervals, validating both the method and the model.

Therefore, under the assumptions outlined above, the function $u(r,t)$ satisfies the conditions required for the existence of a mild solution to Equation (6.1), as established through the fixed-point formulation, spectral representation, or Laplace transformation method. Since the initial condition is given by $u(r,0) = \mathrm{e}^{\phi r}$, which is analytic and sufficiently smooth, the existence of the solution is guaranteed. The uniqueness of the solution follows from the linearity of the Caputo fractional derivative and the properties of the Laplace transform. Suppose there are two solutions $u_1(r,t)$ and $u_2(r,t)$ satisfying the same initial condition. Then their difference $\tilde{u}(r,t) = u_1(r,t) - u_2(r,t)$ are the homogeneous form of Equation (6.1) with zero initial data. Applying the Laplace transform and using the uniqueness of the inverse transform, we conclude that $\tilde{u}(r,\ell) = 0$, and thus $u_1(r,t) = u_2(r,t)$ almost everywhere in the desired domain. This confirms that the solution is unique in the region $[0,r] \times [0,t]$. Hence, the solution $u(r,t)$ to Equation (6.1) with initial condition $u(r,0) = \mathrm{e}^{\phi r}$ is both well-defined and unique, and it depends continuously on the given initial data within the specified domain.

6.5. Comparing the Performance of Analytical Methods in the Fractional Time Diffusion-Reaction Model

In this section, we present a comparative analysis of the three analytical techniques applied to the time-fractional diffusion-reaction model (Equation 6.1): the Homotopy Perturbation Method (HPM), the Fractional Reduced Differential Transform Method (FRDTM), and the Reduced Differential Transform Method (RDTM). Each method offers unique advantages and limitations in terms of analytical tractability, convergence behavior, and computational efficiency.

- **Homotopy Perturbation Method (HPM)**

The HPM constructs the solution as a recursive series expansion. Two approaches are considered: a direct expansion using the Caputo fractional integral operator, and an embedding parameter formulation involving Mittag-Leffler functions. The direct method iteratively generates approximation $u_n(r,t)$, while the embedding parameter approach transforms the PDE into a fractional ODE for the temporal component $w(t)$, solved via nested convolution integrals. This method excels in overseeing nonlinearities and capturing memory effects intrinsic to fractional dynamics. The use of Mittag-Leffler functions allows for accurate modeling of long-time behavior. However, the method becomes increasingly complex with higher-order terms, and the convolution integrals can be analytically demanding.

- **Fractional Reduced Differential Transform Method (FRDTM)**

The FRDTM expresses the solution as a fractional power series in time, where each coefficient $U_k(r)$ is determined recursively. The Caputo derivative and spatial derivatives are transformed into algebraic forms, enabling efficient computation of successive terms. This method is particularly effective for small time intervals due to its rapid convergence and straightforward implementation. It is well-suited for generating low-order approximations and provides clear insight into the influence of fractional dynamics. Nevertheless, the approximation of nonlinear terms such as t^2u may introduce projection errors, and the accuracy can diminish for larger time domains unless higher-order terms are included.

- **Reduced Differential Transform Method (RDTM)**

The RDTM also constructs a fractional power series solution but employs a distinct transformation of the Caputo derivative and utilizes convolution properties to oversee nonlinear terms. The recurrence relations for the coefficients $U_k(r)$ incorporate both spatial derivatives and time-dependent nonlinearities. This method is systematic and capable of recovering the exact classical solution when $\alpha = 1$, providing a useful consistency check. It is particularly effective for problems with analytic initial conditions. However, the method requires careful treatment of convolution terms, and the matching of fractional powers in nonlinear expressions can be technically intricate.

- **Summary**

All three methods provide viable frameworks for approximating solutions to

the fractional diffusion-reaction model. The HPM offers flexibility and depth, especially when leveraging Mittag-Leffler functions. The FRDTM is efficient and rapidly convergent for early-time behavior, while the RDTM provides a structured and consistent approach that bridges classical solutions. The choice among these methods depends on the specific requirements of accuracy, computational resources, and the nature of the problem under consideration.

7. Discussions and Results

To evaluate the performance of different semi-analytical methods in solving the nonlinear partial differential Equation (2.3) we applied the Homotopy Analysis Method (HAM), Homotopy Perturbation Method (HPM), and Reduced Differential Transform Method (RDTM). The resulting approximate solutions are visualized in **Figures 1(a)-(c)**, each plotted over the same spatial and temporal domain. As shown in **Figure 1(a)**, the HAM solution exhibits a smooth and gradual increase in the function $u(r,\tau)$ over time and space. The method constructs a recursive series solution with a convergence-control parameter $\hbar$, which allows flexibility in tuning the approximation. However, due to the nature of the series expansion, the convergence rate is relatively slower compared to the other methods. This is reflected in the surface profile, which remains elevated and continues to evolve throughout the domain. **Figure 1(b)** presents the solution obtained via HPM. This method combines the classical perturbation technique with homotopy theory, yielding a rapidly converging series. In this case, the HPM solution closely matches the exact analytical form $u(r,\tau)=\ln(r+2+\tau)$, resulting in a surface that rises consistently and smoothly. The method demonstrates high accuracy and efficiency, particularly for problems with well-behaved nonlinearities. The RDTM solution, depicted in **Figure 1(c)**, shows a distinct behavior. The surface flattens more quickly than those produced by HAM and HPM, indicating that the method reaches a quasi-steady state earlier. This suggests that RDTM is particularly effective in capturing the early-time dynamics of the system. The method constructs a time-series expansion, which is advantageous for problems where short-time behavior is of primary interest. By comparing these profiles, we can see that each method has distinct advantages and limitations. HPM and RDTM both recover the exact solution, but RDTM stabilizes more rapidly, making it well-suited for early-stage modeling. HAM offers greater flexibility, yet it may require higher-order terms or careful tuning of $\hbar$ to achieve similar accuracy. These insights are valuable for choosing the most appropriate method to model glioma cell dynamics or other nonlinear diffusion-reaction systems. If we observe these profiles over a longer period, we find that the solution evolves smoothly, with the concentration gradually stabilizing as time progresses. This behavior is captured effectively in **Figure 1(d)**, where the Reduced Differential Transform Method (RDTM) is used to compute the solution $u(r,\tau)$ across space and time. The color gradient in the plot from deep blue (low values) to bright yellow

(high values) shows how the solution develops. Notably, the early-time region (lower τ) already displays a well-structured and stable profile, highlighting RDTM's strength in capturing early-stage dynamics. This supports the idea that RDTM stabilizes more rapidly than other methods like HPM or HAM. While HPM also recovers the exact solution, it may require more terms to reach this level of clarity. HAM, on the other hand, offers flexibility through the tuning parameter $\hbar$, but often demands careful adjustment or higher-order expansions to achieve similar accuracy. Additionally, we examined the radius of glial cell concentration to demonstrate the influence of a nonlinear source term $\omega(r,\tau)$ in Equation (2.3). As described in Section 2, this source term incorporates the combined effects of medical treatments such as radiotherapy and chemotherapy into the model. By considering the transformation $\tau = 4D\tau$ from relation (2.4) and setting the diffusion coefficient $D = 2.5$ along with the number of glial cells $N = 8000$ (as referenced in [11]), we obtain the values listed in **Table 1**. Using these values, **Figure 2** is generated, which shows that the radius of glioma cells decreases over time. **Figures 3(a)-(d)** present the concentration profiles of glial cells derived from the fractional Equation (6.1) using the Homotopy Perturbation Method (HPM) at successive approximation orders: u_0, u_1, u_2, and u_3. These visualizations illustrate the first, second, and third-order approximations, each capturing increasingly detailed dynamics of the solution. With extended time, range and enhanced contrast, the progressive evolution of the surface becomes more pronounced. The first-order approximation u_1 introduces initial curvature and a subtle dip near the origin, reflecting the early influence of the nonlinear term $-t^2u$. The second-order approximation u_2 deepens this effect, while the third-order approximation u_3 reveals even greater curvature and complexity, highlighting the refined behavior of the solution as it diverges from the initial flat profile u_0. These figures not only emphasize the recursive structure of the HPM series but also demonstrate the method's strong and rapid convergence. Although the differences between successive approximations (u_0 to u_3) may appear subtle, this is due to the smoothing effect of the fractional derivative and the inherent efficiency of the HPM. The color gradients in the 3D surface plots clearly indicate a consistent decrease in glioma cell concentration over time, with each higher-order approximation reinforcing this downward trend. We can also conclude that the profiles exhibit a progressive decay toward zero, suggesting that the HPM effectively models the suppression or eventual cessation of glial cell growth. **Figure 4** further supports this interpretation by illustrating the impact of the fractional time derivative on glial cell concentration for the third-order approximate solution at $r = 0.1$, using various values of the fractional order $\alpha = 1.5; 1.25; 0.75; 0.5$ and 0.5. As α decreases, the decay in cell concentration becomes more gradual, underscoring the role of memory effects inherent in fractional-order systems. This behavior confirms that the fractional derivative not only smooths the temporal evolution but also significantly influences the rate and pattern of glioma cell suppression. Together, these results reinforce

the flexibility and effectiveness of the HPM in capturing the complex dynamics of biological systems governed by fractional differential equations. Under the given conditions, the concentration of glioma cells decreases as the fractional order decreases from $\alpha = 1.5$ to $\alpha = 0.5$. This indicates that a fractional derivative of order $\alpha = 0.5$ is more effective in reducing glial cell concentrations. **Figures 5(a)-(d)** illustrate the evolving behavior of the solution surface as higher-order corrections are introduced through the fractional reduced differential transform method (FRDTM). From **Figures 5(a)-(d)**, the surface exhibits a progressively sharper dip near the origin, especially as time increases. Unlike the gentle slope seen in **Figure 5(b)** (u_1), the later subfigures show the surface bending downward more steeply and earlier in time. The color gradient shifts more rapidly, transitioning from yellow to deep blue, which indicates a faster and stronger decrease in cell concentration. This transformation is driven by the inclusion of second- and third-order corrections. In **Figure 5(c)**, the second-order term enhances the curvature, intensifying the effects of the fractional derivative and the nonlinear $-t^2u$ term. By **Figure 5(d)**, the third-order correction further amplifies these influences, resulting in a more pronounced twisting of the surface and a wider dynamic range in the color map highlighting lower concentrations reached more quickly and a stronger decay pattern overall. To clearly illustrate the progressive changes in the solution behavior, a 2D profile of the FRDTM-based approximations u_0 through u_3 is shown in **Figure 5(e)**. This visualization highlights the convergence trend and the influence of higher-order terms more effectively than the 3D surfaces. Comparing **Figure 5** and **Figure 3**, we observe that the fractional model exhibits faster convergence when solved using the FRDTM method. **Figure 6** shows a clear and compelling visual confirmation of the theoretical results derived through the sectorial operator framework and the Mittag-Leffler function representation for the fractional differential Equation (6.1). The smooth and well-structured surface of the solution $u(r,t)$ illustrates the three fundamental properties of existence, uniqueness, and stability. The continuity and boundedness of the surface across the domain $(r,t) \in [0,3] \times [0,10]$ demonstrate the existence of a mild solution $u \in C([0,T];X)$, consistent with the analytic initial condition $u(r,0) = e^{\phi r}$, which lies in the domain of the sectorial operator A. The absence of irregularities or bifurcations in the surface supports the uniqueness of the solution, as ensured by the structure of the Volterra-type integral equation and the properties of the two-parameter Mittag-Leffler operator function. Moreover, the smooth decay of the solution over time, clearly visible in the surface's downward trend, confirms the solution's stability. This behavior aligns with the derived a priori bounds and the application of the fractional Grönwall inequality, which guarantee that the solution depends continuously on the initial data and remains well-behaved over time. These visual and analytical insights validate the model and further support the use of numerical methods such as FRDTM for constructing accurate approximations to the solution.

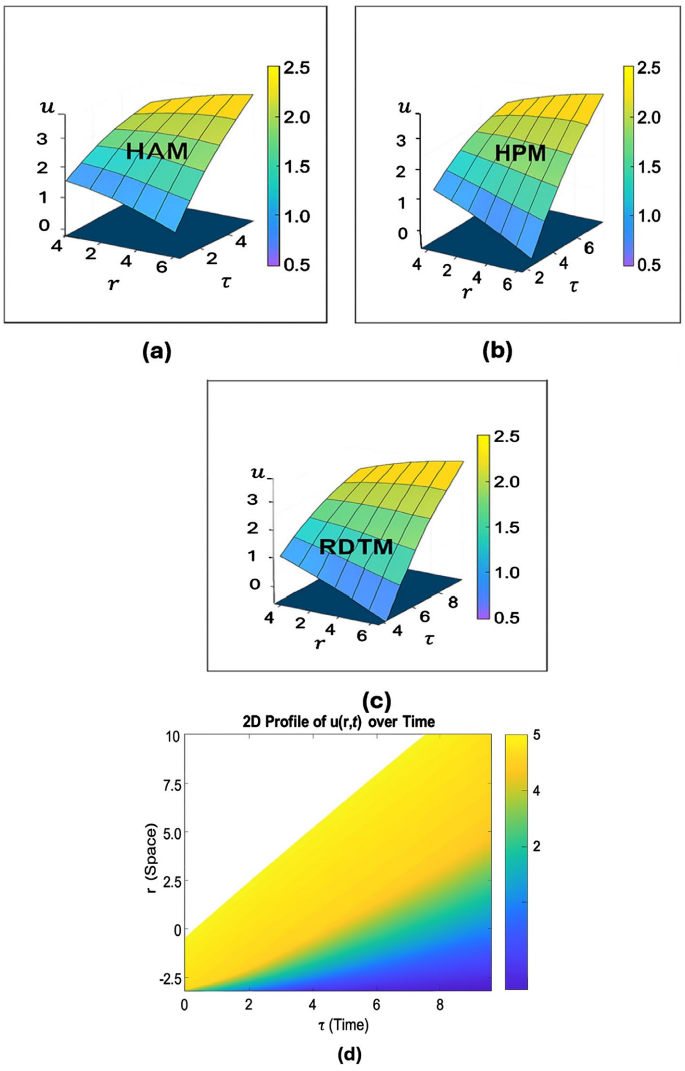

Figure 1. (a)-(c): Cell concentration profiles obtained by solving Eq. (2.3) using the HAM, HPM, and RDTM methods over the domain $u(r,\tau)\in(0,r]\times[0,\tau]$ for $\alpha=0.5$; (d): two-dimensional spatiotemporal profile of $u(r,\tau)$ computed using RDTM over time.

Table 1. Radial growth of glial cells in the treated model.

Radius of Glial Cells	
τ (time)	r (radius)
1	5.75
2	5.25
3	4.75
4	4.25
5	3.75
6	3.25

Continued

7	2.75
8	2.25
9	1.75
10	1.25

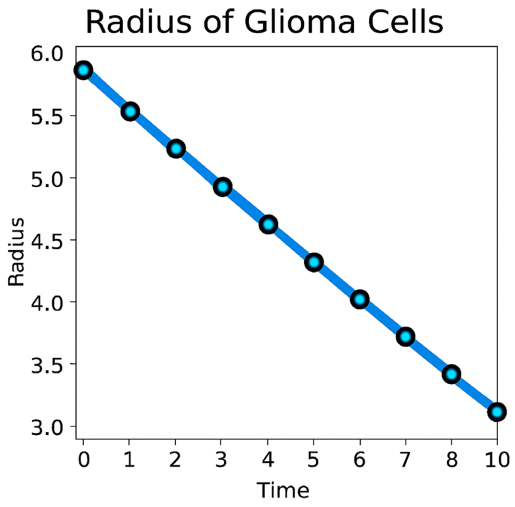

Figure 2. Radial growth of glial cells over the time interval $\tau \in [0,10]$.

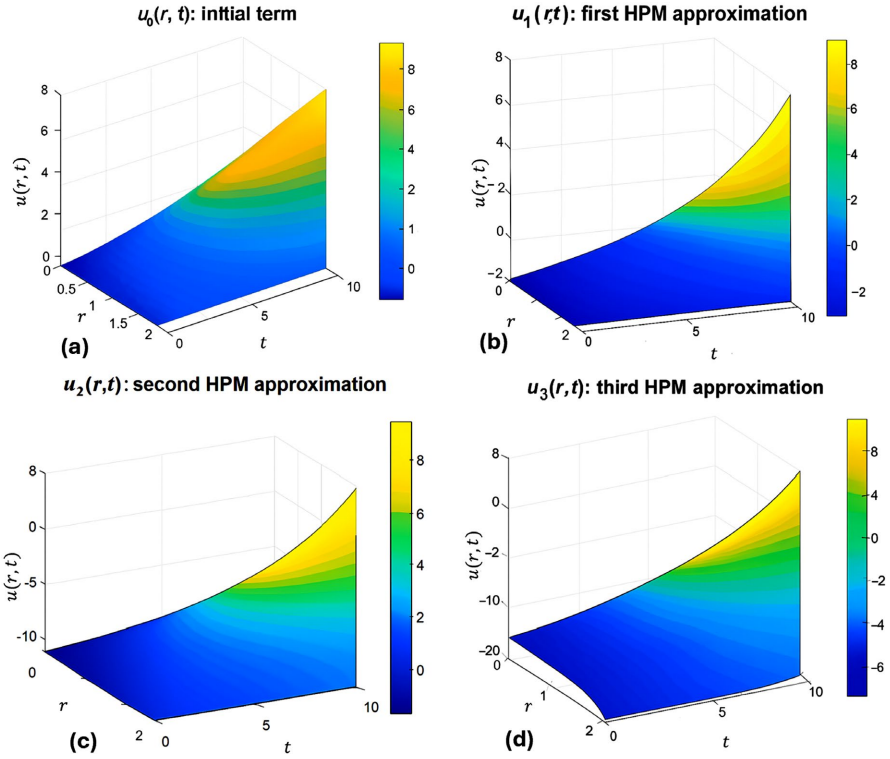

Figure 3. Cell concentration profiles obtained from the solution of Eq. (6.1) using the Homotopy Perturbation Method (HPM) at $\alpha = 0.5$: (a) u_0, (b) u_1, (c) u_2, (d) u_3.

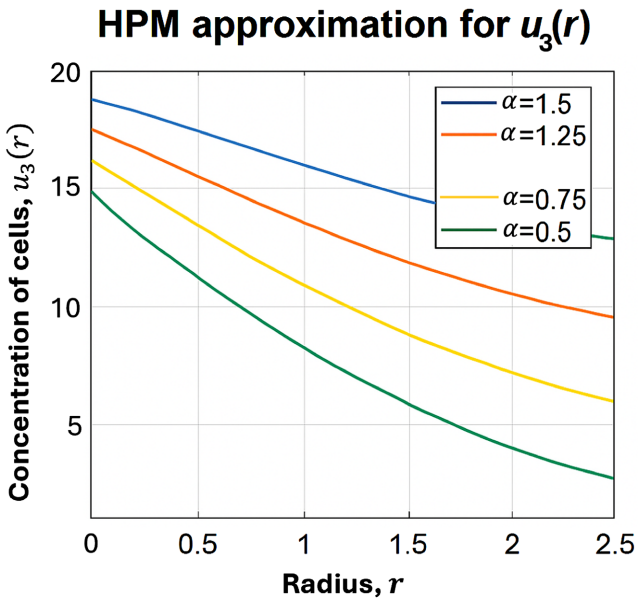

Figure 4. Effect of the fractional-order parameter α on cell concentration in the third-order approximation u_3 of Eq. (6.1), obtained using the Homotopy Perturbation Method (HPM), for $\alpha = 1.5, 1.25, 0.75, 0.5$.

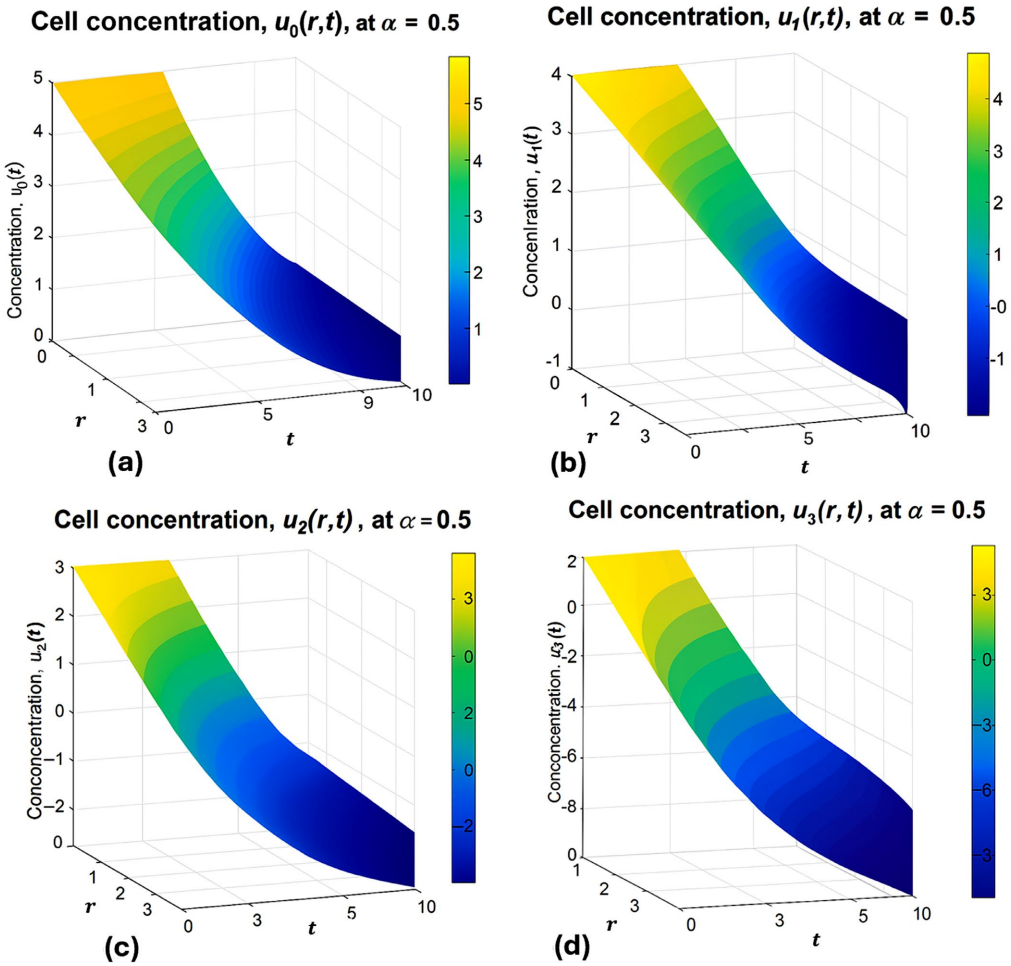

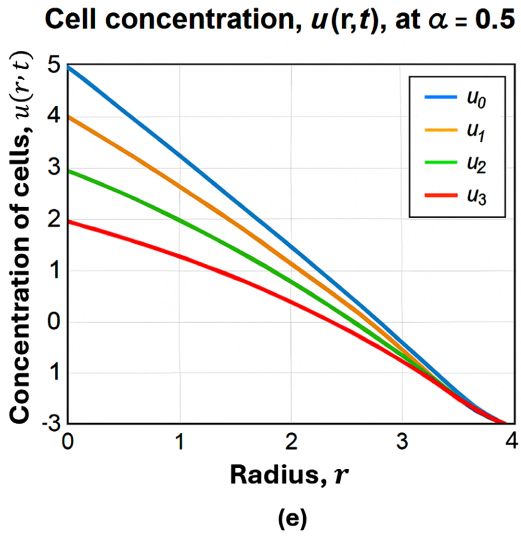

Figure 5. (a)-(d) Cell concentration profiles corresponding to the approximate solutions u_0, u_1, u_2, u_3 of Eq. (6.1) obtained using FRDTM; (e) Two-dimensional plot of the cell concentration for $\alpha = 0.5$, also computed via FRDTM.

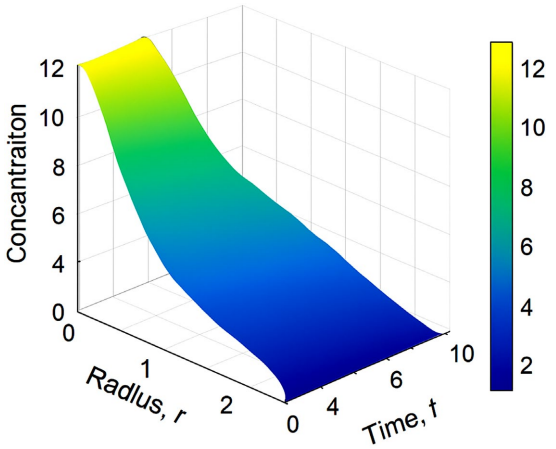

Figure 6. Plot of the mild solution to Eq. (6.1) for $\alpha = 0.5$, illustrating existence, uniqueness, and stability of the fractional model via the Mittage-Leffler function.

8. Conclusion

In this work, the dynamics of a nonlinear glial cell growth model under treatment were examined using three analytical methods HAM, HPM, and RDTM to derive approximate solutions. The resulting growth profiles confirmed the effectiveness of these approaches in tackling complex partial differential equations, with RDTM standing out for its superior efficiency and accuracy. Analysis of the glioma cell radius showed a consistent decline over time, emphasizing the impact of treatment parameters in suppressing glioma expansion. By extending the model to its fractional form, we established the existence and uniqueness of the solution and simulated its behavior. The three-dimensional solution profiles revealed a steady decrease in glial cell concentration, ultimately reaching zero, indicating complete growth suppression. Among the fractional parameters tested, $\alpha = 0.5$ proved most

effective in accelerating the decline, highlighting the significance of fractional derivatives in enhancing model precision and therapeutic insight. Overall, these findings underscore the power of fractional modeling in capturing the complex behavior of biological systems and offer valuable guidance for developing more effective treatment strategies.

Conflicts of Interest

The author declares no conflicts of interest regarding the publication of this paper.

References

[1] Lassaletta, A., Zapotocky, M., Bouffet, E., Hawkins, C. and Tabori, U. (2016) An Integrative Molecular and Genomic Analysis of Pediatric Hemispheric Low-Grade Gliomas: An Update. *Child's Nervous System*, **32**, 1789-1797. https://doi.org/10.1007/s00381-016-3163-6

[2] Melian, E. (2014) Radiation Therapy in Neurologic Disease. *Handbook of Clinical Neurology*, **121**, 1181-1198.

[3] Lloret-Villas, A., Varusai, T., Juty, N., Laibe, C., Le NovÈre, N., Hermjakob, H., *et al.* (2017) The Impact of Mathematical Modeling in Understanding the Mechanisms Underlying Neurodegeneration: Evolving Dimensions and Future Directions. *CPT*: *Pharmacometrics & Systems Pharmacology*, **6**, 73-86. https://doi.org/10.1002/psp4.12155

[4] Einevoll, G.T. (2006) Mathematical Modeling of Neural Activity. In: Skjeltorp, A.T. and Belushkin, A.V., *Dynamics of Complex Interconnected Systems*: *Networks and Bioprocesses*, Springer, 127-145.

[5] Nijhout, H.F., Best, J.A. and Reed, M.C. (2015) Using Mathematical Models to Understand Metabolism, Genes, and Disease. *BMC Biology*, **13**, Article No. 79. https://doi.org/10.1186/s12915-015-0189-2

[6] Georgescu, M., Haidar, L., Serb, A., Puscasiu, D. and Georgescu, D. (2021) Mathematical Modeling of Brain Activity under Specific Auditory Stimulation. *Computational and Mathematical Methods in Medicine*, **2021**, 1-20. https://doi.org/10.1155/2021/6676681

[7] Wein, L. and Koplow, D. (1999) Mathematical Modeling of Brain Cancer to Identify Promising Combination Treatments. https://www.virtualtrials.com/weinrep2.pdf

[8] Tracqui, P., Cruywagen, G.C., Woodward, D.E., Bartoo, G.T., Murray, J.D. and Alvord, E.C. (1995) A Mathematical Model of Glioma Growth: The Effect of Chemotherapy on Spatio-Temporal Growth. *Cell Proliferation*, **28**, 17-31. https://doi.org/10.1111/j.1365-2184.1995.tb00036.x

[9] Woodward, D.E., Cook, J., Tracqui, P., Cruywagen, G.C., Murray, J.D. and Alvord, E.C. (1996) A Mathematical Model of Glioma Growth: The Effect of Extent of Surgical Resection. *Cell Proliferation*, **29**, 269-288. https://doi.org/10.1111/j.1365-2184.1996.tb01580.x

[10] Stupp, R., Mason, W.P., van den Bent, M.J., Weller, M., Fisher, B., Taphoorn, M.J.B., *et al.* (2005) Radiotherapy Plus Concomitant and Adjuvant Temozolomide for Glioblastoma. *New England Journal of Medicine*, **352**, 987-996. https://doi.org/10.1056/nejmoa043330

[11] Gonzalez-Gaxiola, O. and Bernal-Jaquez, R. (2017) Applying Adomian Decomposition Method to Solve Burgess Equation with a Non-Linear Source.

https://arxiv.org/abs/1606.00259

[12] Iyiola, O.S. and Zaman, F.D. (2014) A Fractional Diffusion Equation Model for Cancer Tumor. *AIP Advances*, **4**, Article 107121. https://doi.org/10.1063/1.4898331

[13] Carpio, A. and Bonilla, L.L. (2012) Modeling Tumor Growth: A Review of Continuum Models. *Applied Mathematics Letters*, **25**, 1374-1380.

[14] Bonilla, L., Carpio, A. and Bernal, R. (2013) Modeling and Simulation of Glioma Growth. *Mathematical Models and Methods in Applied Sciences*, **23**, 1089-1118.

[15] Liao, S. (1997) A Kind of Approximate Solution Technique Which Does Not Depend Upon Small Parameters—II. An Application in Fluid Mechanics. *International Journal of Non-Linear Mechanics*, **32**, 815-822. https://doi.org/10.1016/s0020-7462(96)00101-1

[16] Liao, S. (2004) On the Homotopy Analysis Method for Nonlinear Problems. *Applied Mathematics and Computation*, **147**, 499-513. https://doi.org/10.1016/s0096-3003(02)00790-7

[17] Abbasbandy, S. (2007) The Application of Homotopy Analysis Method to Solve a Generalized Hirota–satsuma Coupled KDV Equation. *Physics Letters A*, **361**, 478-483. https://doi.org/10.1016/j.physleta.2006.09.105

[18] Chakraverty, S., Mahato, N., Karunakar, P. and Rao, T.D. (2019) Homotopy Analysis Method. Wiley, 149-156. https://researchgate.net/publication/364676137

[19] He, J.H. (1999) Homotopy Perturbation Technique. *Computer Methods in Applied Mechanics and Engineering*, **178**, 257-262. https://doi.org/10.1016/s0045-7825(99)00018-3

[20] He, J.H. (1999) Variational Iteration Method—A Kind of Non-Linear Analytical Technique: Some Examples. *International Journal of Non-Linear Mechanics*, **34**, 699-708. https://doi.org/10.1016/s0020-7462(98)00048-1

[21] He, J.H. (2006) Some Asymptotic Methods for Strongly Nonlinear Equations. *International Journal of Modern Physics B*, **20**, 1141-1199. https://doi.org/10.1142/s0217979206033796

[22] Zhou, J.K. (1986) Differential Transform and Its Applications for Electrical Circuits. Huazhong University Press. https://www.scirp.org/reference/referencespapers?referenceid=1912818

[23] Gareema, P.V. and Agarwal, G. (2024) Reduced Differential Transform Method and Its Applications. Indian National Science Academy.

[24] Jafari, H., Jassim, H.K., Moshokoa, S.P., Ariyan, V.M. and Tchier, F. (2016) Reduced Differential Transform Method for Partial Differential Equations within Local Fractional Derivative Operators. *Advances in Mechanical Engineering*, **8**, 1-6. https://doi.org/10.1177/1687814016633013

[25] Patel, H.S. and Patel, T. (2021) Applications of Fractional Reduced Differential Transform Method for Solving the Generalized Fractional-Order FitzHugh-Nagumo Equation. *International Journal of Applied and Computational Mathematics*, **7**, Article 188. https://doi.org/10.1007/s40819-021-01130-2